BLM LIBRARY
88001689

jpl

A STUDY TO DETERMINE THE FEASIBILITY OF USING RADAR TECHNIQUES FOR PUBLIC LAND SURVEYING

1200-214 May 20, 1975

JET PROPULSION LABORATORY
CALIFORNIA INSTITUTE OF TECHNOLOGY
PASADENA, CALIFORNIA

HD
216
.B52

Bureau of Land Management
Library
Bldg. 50, Denver Federal Center
Denver, CO 80225

#319561
ID 88001689

HD
216
.B52

Bureau of Land Management
Library
Bldg. 50, Denver Federal Center
Denver, CO 80225

A STUDY TO DETERMINE THE FEASIBILITY OF USING RADAR TECHNIQUES FOR PUBLIC LAND SURVEYING

1200-214 May 20, 1975

Submitted
to

U.S. DEPARTMENT OF INTERIOR
BUREAU OF LAND MANAGEMENT
Scientific Systems Development Office
Denver Service Center
Denver, Colorado 80225

BLM P.O. No. 53500-PH3-995

Prepared
by

Thomas Bicknell
Gunther H. Redmann
Walter E. Brown, Jr.

Bureau of Land Management
Library
Bldg. 50, Denver Federal Center
Denver, CO 80225

JET PROPULSION LABORATORY
CALIFORNIA INSTITUTE OF TECHNOLOGY
PASADENA, CALIFORNIA

BUREAU OF LAND MANAGEMENT LIBRARY
Denver, Colorado
88001689

ACKNOWLEDGMENTS

This study was developed as a result of the combined efforts of Mr. Grover Torbert, Bureau of Land Management, Washington, D. C., and persons from the Bureau of Land Management, Portland Service Center.

Special acknowledgment is given to Dale Bedell and Bill Ball (now at the Denver Service Center) for their invaluable aid in finding an appropriate site for this test and in arranging the logistic support, site survey and target deployment.

The site development and survey work and deployment and recovery of targets was performed by Mike Gardner, Ron Scherler and George Huggins with the help of Mike Blackwell, Dick Bidasolo and Fred Sawyer. We are indebted to them for their excellent field support.

CONTENTS

SECTION

I. INTRODUCTION 1
A. BACKGROUND 1
B. SCOPE 2
C. OBJECTIVES 2
II. TECHNICAL DISCUSSION 3
A. DESCRIPTION OF EXPERIMENT 3
1. Target Site 3
2. Flight Path 6
3. Radar Description 6
4. Data Reduction. 7
B. RADAR SYSTEM CALCULATIONS. 9
1. Range and Azimuth Resolution 9
2. The Detection of Passive Reflectors 10
3. Scintillation Effects 11
4. Ranging Accuracy and Range Calculations 12
III. DATA ANALYSIS AND RESULTS 17
IV. ALTERNATE TARGET CONSIDERATIONS 21
V. CONCLUSIONS 25

APPENDIXES

A. RADAR DESCRIPTION AND RADAR SIGNAL FILM CHARACTERISTICS 27
B. PROCESSOR THEORY AND OPERATION 37
C. A SECOND HARMONIC TRANSPONDER 57

FIGURES

1. Rock Creek Reservoir, Mt. Hood National Forest, showing selected target site 4
2. Target site 5
3. Cartesian coordinate system 15
4. Enlargements of radar imagery 19
5. Passive transponder 22

SUMMARY

The Bureau of Land Management (BLM) is investigating various remote sensing and locating systems to determine if any of the current, state-of-the-art, airborne systems are suitable, or readily adaptable, for public land surveying in forested areas or where persistent cloud cover occurs.

This study investigated the use of radar ranging techniques for locating and establishing corner markers for public land surveys under these conditions. Passive reflectors with radar cross-sections 3 to 6 dB greater than the average terrain cross-section were deployed in an Oregon test site. The test site was imaged with an L-band synthetic aperture radar mounted on the NASA Ames CV-990 aircraft. Surface features in the test site area were imaged but the reflectors were not identified in the imagery. The scintillation (favorable phase addition) from the irregular surface was greater than the reflector signal strength.

SECTION I

INTRODUCTION

A. BACKGROUND

As the result of presentations made at the Jet Propulsion Laboratory (JPL) of the California Institute of Technology to representatives of the EROS Project Office in 1972 of remote sensing techniques developed for NASA, BLM expressed interest in pursuing the possibility of using the coherent, side-looking radar system (SLAR) developed for the Apollo Applications Project as a range determining instrument for use in public land surveying. A major problem which the Cadastral Survey Branch of BLM has is to efficiently survey public lands in heavily forested areas or in regions where fog and clouds generally obscure the ground.

Several meetings were held with BLM to review the specific ranging accuracy and variable foliage or tree density penetration requirements to establish if the accuracy and "penetration" capabilities of this type radar system could be applicable to this problem. Preliminary signal-to-noise (background clutter) calculations were made and it was decided to provide R&D support to BLM using existing equipment for determining the feasibility of using radar ranging techniques for locating and establishing corner markers for public land surveys in forested areas.

Arrangements were made with NASA to use the CV-990 aircraft to fly a BLM test site on a non-interference basis at such time as the JPL 25 cm, coherent SLAR system was already installed on the aircraft for other experiments. The crash of the original CV-990 in April, 1973 caused almost a one-year delay in this program and had great impact in the subsequent planning and execution of a cohesive and efficient study.

Three sites were tentatively selected by BLM which provided exposed known reference corners and the proper forest cover for this experiment. Joint

site visits were made and a site southeast of Mt. Hood was selected for ease of target deployment and site surveying while offering representative forest cover and flight path clearance.

B. SCOPE

Two overflights were planned in an orthogonal pattern so that north-south ranging would be done on one leg and east-west ranging would be done on the second leg. JPL procured several radar reflectors (Luneberg reflectors) of a size believed adequate to provide a sufficient signal strength under the severe conditions of variable forest density assumptions and also some 18-in. reflectors used in other experiments. The imagery obtained from the overflights was processed to determine the ability to locate the corners and establish horizontal distances between corners to the desired accuracy.

C. OBJECTIVES

Several objectives were established for this study, each dependent for its accomplishment upon the successful completion of the preceding objective.

1) Establish that a coherent radar system with proper parameters will discriminate corner markers through forest cover.
2) Determine the software and computer support required to achieve the desired survey accuracy.
3) Develop concepts for an economical, easily deployable, radar target(s) for use as corner markers.

SECTION II

TECHNICAL DISCUSSION

A. DESCRIPTION OF EXPERIMENT

1. Target Site

The prime consideration in choosing a site was its suitability in determining whether or not a lens could be seen under the cover of a wooded area. Other considerations were ease of deployment and avoidance of large elevation changes in or near the site area. The ideal area would be one which included a stand of trees next to relatively open and flat fields. Thus a pattern of lenses could be positioned so that some were plainly visible in the open field, and a lens in the trees could be located with respect to them.

An area was found in the Mt. Hood National Forest in Oregon. The site was approximately one mile north of Rock Creek Reservoir, which served as an identifying geographical feature both to the navigator on the aircraft and in the radar imagery. Figure 1 shows a topographic map of the area with the approximate location of the targets sketched in. As shown in Fig. 2, a rectangle with a 2000-ft length (east to west) and 1000-ft width (north to south) was laid out so that the soutwest corner was situated in a stand of trees while the other corners were in open fields. The 36-in. reflector was placed at this corner and the two 24-in. lenses were arrayed on a line intersecting the 36-in. lens. The purpose of this formation was to aid in locating the large reflector in the data and to test the geometric correction program in the digital processing system. Additionally a 12-in. and an 18-in. lens were located along the sides of the rectangle in the wooded area to determine if smaller reflectors would be visible to the radar through the cover of the trees.

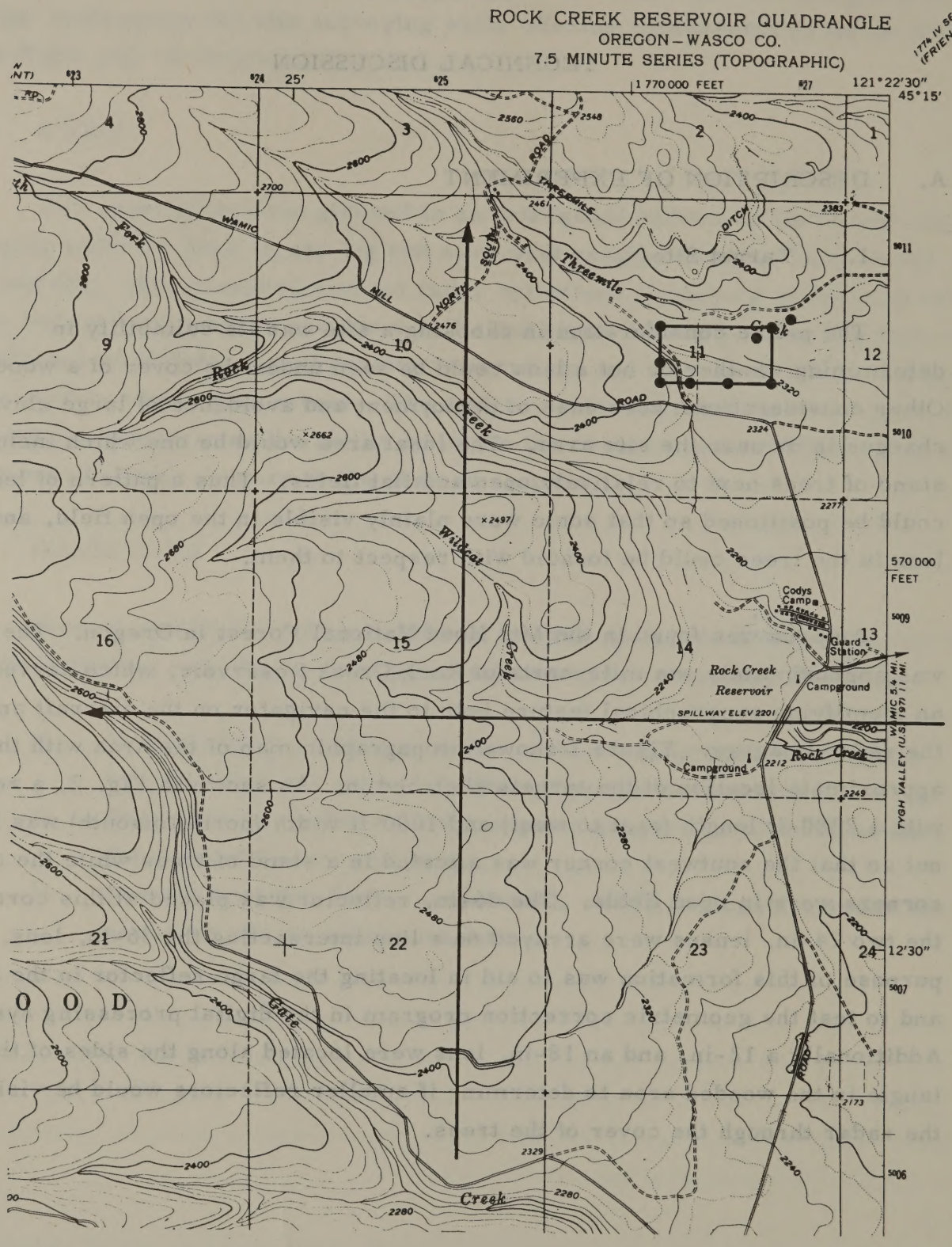

Fig. 1. Rock Creek Reservoir, Mt. Hood National Forest, showing selected target site

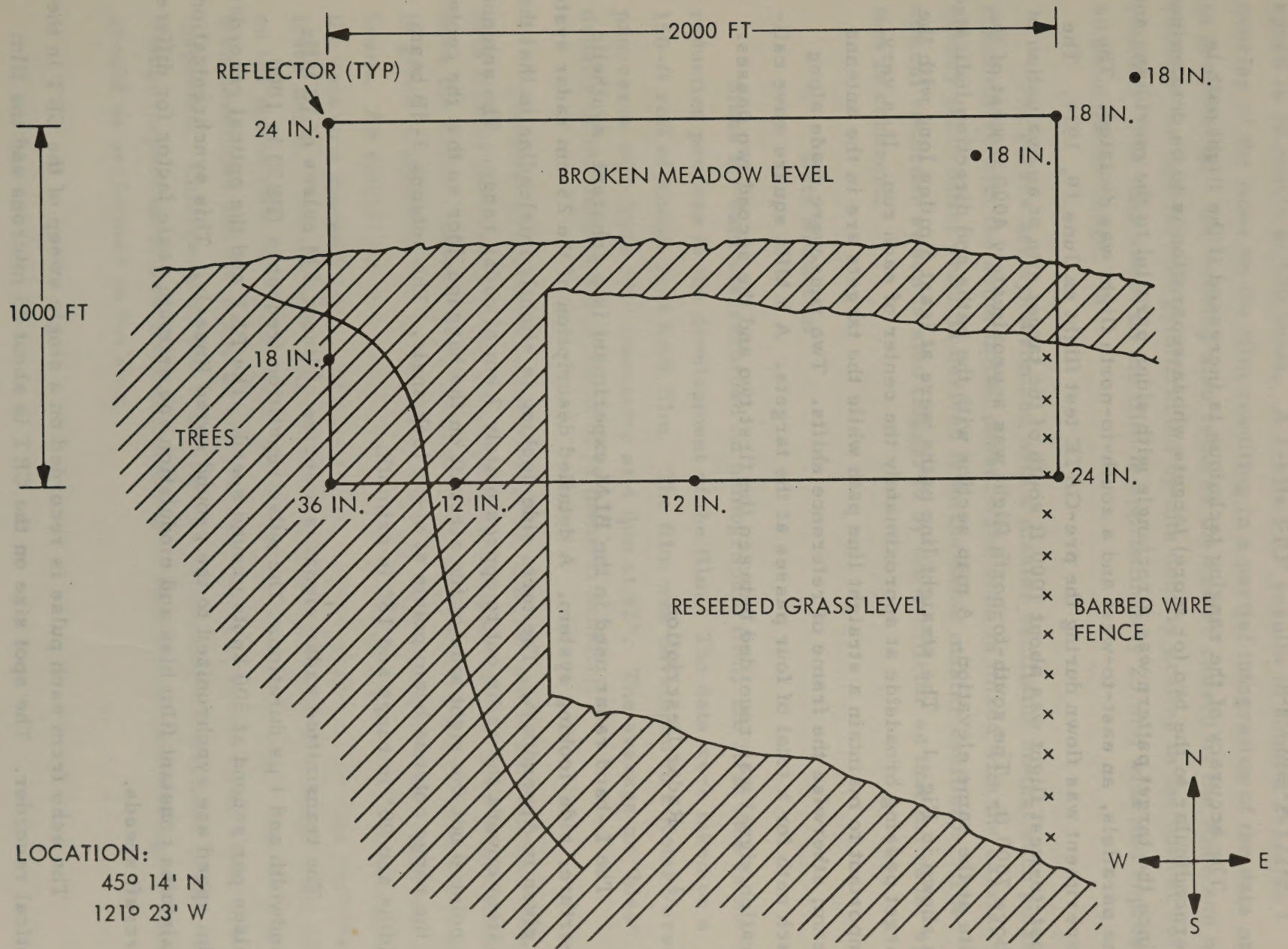

Fig. 2. Target site

2. Flight Path

The accuracy of the ranging technique is increased if the flight path is perpendicular to the two (or more) targets whose separation is to be determined. Since the target pattern was a rectangle with sides parallel to the meridians and the parallels, an east-to-west and a south-to-north flight was dictated. The experiment was flown during the pre-GATE test flight on June 19, 1974. The east-to-west flight was about 7000 ft south of the target site at an evaluation of above 7000 ft. The south-to-north flight was approximately 4000 ft west of the site at the same elevation. A map section with the paths and direction indicated is shown in Fig. 1. The straight line paths were at least 5 miles long with the target passing broadside at approximately the center of each run. It is very important to maintain a straight line path while the targets are in the antenna beam; otherwise the frame of reference shifts. Two runs were made along each path for a total of four passes at the targets. A 5 MHz square wave calibration signal was recorded between the first two and the second two passes.

3. Radar Description

The L-band radar used in the BLM experiment is a coherent, synthetic aperture, side-looking system. A detailed description of the 25-cm radar system is given in Appendix A. The term side-looking is slightly misleading in that the system covers the nadir out to approximately 7 km of radar range. The antenna is pointed out the right side of the aircraft on the baggage door so that the center of the range antenna beam points at a 45° look angle. The antenna 3-dB beam widths are 90° in range and 18° in azimuth.

The transmitted radar signal is a series of linear FM pulses of 10 MHz bandwidth and 1 μs duration. The pulse repetition frequency (PRF) is 1000 pulses per second at 500 knots ground speed. The PRF and the optical recorder film speed are synchronized to the ground speed linearly. This synchronization maintains constant film bias and modulation and azimuth scale factor for different aircraft speeds.

The echo from each pulse is recorded on a single sweep of the CRT in the optical recorder. The spot size on the CRT is about 25 microns and the film

speed is 10 mm/s at 500 knots. A 1-kHz PRF results in about a 2-1/2 to 1 overlap of the lines on the film resulting in a partial integration of the data prior to processing. The overlap also reduces the raster caused by the lines and hence reduces the optical energy diffracted by this density grating in the optical correlator. The data swath on the film is approximately 25 mm wide and represents 50 μs of radar range.

The pulses are synchronized with a master oscillator so that each pulse is transmitted with the same initial phase. The echo is mixed with the carrier frequency (1215 MHz) which is derived from the same master oscillator. The optical recorder sweep is also triggered by the oscillator so that the radar system is coherent.

4. Data Reduction

Since the data are recorded on photographic film, the first step in the data reduction process is the development of the film. The data were taken on a 150-ft roll of Kodak 3493 RAR film. The film was developed in a Kotal Versamat processor with Type "A" chemistry at 4 fpm at 82°. The average or "bias" density of the data swath is about 0.38 (neutral density).

The first processing performed on the data is optical correlation. The data film is processed by the JPL optical correlator one or more times to produce the radar images. A detailed description of the optical correlation process is given in Appendix B. In summary the film is illuminated with a coherent laser beam. An optical system composed of spherical and cylindrical lenses focuses the data to a planar image. The input film drive transports the data past the laser beam. The focused image at the output is recorded by photographic film on the output film drive moving in synchronism with the image. The film is then developed and the areas of interest, in this case the test site area, are inspected. Enlargements are made to aid in analyzing a particular image area. Visual inspection allows the determination of what digital processing, if any, should be performed on the data.

Digital processing may be performed on either a correlated radar image or the original data. The optical-to-digital interface which converts the video data to magnetic tape is a scanning microdensiter (CVFR) run by a PDP-11 computer. A photographic transparency is converted to a digital matrix with the X-Y coordinates and the density or transmission value of each point in the picture. The CVFR (continuous video film recorder) has a 10-micron spot-size capability with a 1-micron accuracy in coordinate location. The data are digitized in a manner similar to their recording, with continuous scans made across the swath in the range direction. Once the data are digitized on magnetic tape, the digital correlation process, geometric correction, etc. may be performed.

The data must be stretched in range to achieve a geometrically correct image. The radar geometry produces data which are compressed in near-range according to the equation

$$Y_g = \frac{Y_f K_r}{\sin \theta}$$

where Y_g is the true ground distance coordinate, Y_f is the film distance corresponding to that area, K_r is the range scale factor (at the horizon), and θ is the slant angle from straight down. The image is digitized into an array in the computer, stretched, and reprinted so that

$$Y_g = K_r Y_f'$$

where Y_f' is the distance on film after processing.

The basic technique used to determine the distance between two targets in range is to perform a one-dimensional correlation of the data. The data are scanned and digitized, Fourier transformed, multiplied by the "matched filter" for the chirp function, inverse transformed, and printed out either in numbers or on a graph. The matched filter is generated from the chirp function itself as measured on the film. The one-dimensional correlation is performed on each line scanned in the range direction. A scan in azimuth is made first to determine the center of the doppler phase histories of the two targets. The distance of the scan from the phase centers of the two targets is also required to compute their

relative distances. As outlined below in Section II-B-3, the ground range distances can be calculated from the radar range and altitude information obtained from the data.

B. RADAR SYSTEM CALCULATIONS

1. Range and Azimuth Resolution

The ground range resolution of the radar system is

$$r = \frac{C}{2B \sin \theta}$$

where C is the speed of light, B is the pulse bandwith and θ is the angle of the target(s) off vertical. For a bandwidth of 10 MHz and look angle of 30°,

$$r \approx 26 \text{ meters}$$

This is the range spot size which may be degraded or improved by the presence or absence of clutter respectively.

The azimuth resolution is found from the radar wavelength λ and the half-angle of antenna beam in azimuth Φ by

$$a = \frac{2\lambda}{\tan \Phi}$$

The half-angle should be limited by the fact that the recorder MTF (modulation transfer function) is limited to about 30 lines/mm in azimuth or about 300 Hz of Doppler. At a ground speed of 250 meters/s 300 Hz of Doppler will occur at an angle of about 9° which happens to be the antenna half-angle of the L-band radar system anyway. Azimuth resolution is also limited by deviations from flight path or changes in ground speed by the aircraft, while the target is in the antenna beam.

2. The Detection of Passive Reflectors

Luneberg reflectors were used as the targets. The cross-section of the reflector with radius R at wavelength λ is given by

$$\sigma = \frac{4\pi^3 R^4}{\lambda^2}$$

assuming no losses in the dielectric material.

For λ = 25 cm the corss-sections of various lenses used in the experiment are listed below.

Diameter, in.	Cross-section, m^2
12	1
18	5.4
24	17
36	86

These areas are the sizes of a perfect scatterer that would reflect the same energy back to the radar source as the lens reflects.

The cross-section of the surface is found from resolution of the system. The effective resolution of the processed image was approximately 3 meters in azimuth by 26 meters in range or 78 $meters^2$. The normalized radar cross-section (with respect to a perfect scatterer) for a look angle of 30 degrees off vertical is

Forest	0.5
Fields	0.05

So the radar cross-section is

Forest	39 $(meters)^2$	36-in. reflector	86 m^2
Field	4 $(meters)^2$	24-in. reflector	17 m^2

and the detectability

$$\psi_T = \frac{\sigma_{36}}{\sigma_T} = 2$$

$$\psi_F = \frac{\sigma_{24}}{\sigma_T} = 4$$

This ratio could have been increased by increasing the bandwidth of the radar. In general,

$$\psi = \frac{4\pi^3 R^4}{\lambda^2} \cdot \frac{2\beta}{C} \tan\theta \cdot \frac{K}{\sigma}$$

So we can see that the detectability ψ increases with $1/\lambda$, R, β, $\tan\theta$ and $1/\sigma$; however, there are some practical limits. As λ becomes small the dielectric losses limit the value of ψ as θ approaches 90°, the reflector moves to the horizon or farther in range. A small value of σ signifies a flat surface.

3. Scintillation Effects

The echo from any resolution cell that contains surface features such as trees or perturbations which are large with respect to a radar wavelength will consist of a sum of echoes from facets favorably oriented. Since the resolution cell is large with respect to a wavelength these contributions are of random phase (essentially a uniform distribution) and the resultant echo amplitude has a Rayleigh distribution with a value of average-to-deviation of

$$\frac{\overline{X}}{\sigma} = \sqrt{\frac{\pi}{2}}$$

By averaging adjacent resolution cells (N of them) this ratio becomes

$$\frac{\overline{X}}{\sigma} \simeq \sqrt{\frac{\pi N}{2}}$$

In order to achieve a particular accuracy in locating the reflectors, the radar must have an excess resolution capability to provide a reasonable probability that the reflector echo will exceed the peaks of the scintillating echo in

a given area of view. As an example, consider a case when the reflector echo power is

$$(\overline{S})^2 = 4(\overline{X})^2$$

four times the average clutter. Also, the location of the reflector is unknown within a 100 meter square and the location resolution desired is within 1/2 meter rms. Then the single-cell distribution is a Rayleigh distribution with the target echo amplitude twice that of the average clutter.

Let us also assume we would like a probability of successful detection of 0.9. So we need to reduce the variance of the single-cell distribution so that the probability of the clutter exceeding the reflector echo per cell is approximately

$$P(C) \simeq \frac{0.1}{(200)(200)} = \frac{10 \cdot 10^{-2}}{4 \cdot 10^4} = 2.5 \cdot 10^{-6}$$

so the required SNR

$$= \frac{\overline{X}}{\sigma} = 4.9.$$

Then $(4.9)^2 = \frac{\pi N}{2}$ or $N = 15$ = number of looks per 1/2 by 1/2 meter cell, or the radar resolution must therefore be on the order of 1/8 by 1/8 meter.

Of course, if S is much larger than $\overline{X}$ the problem is simplified (i.e., $\overline{S} = 5\overline{X}$; $(\overline{S})^2 = 25(\overline{X})^2$ or 14 dB above the average clutter, then no excess resolution is required). This discussion essentially boxes the problem for the detection of a surface reflector or transponder operating at the interrogation frequency.

4. Ranging Accuracy and Range Calculations

Several factors affect the ranging accuracy of the radar system. The basic system accuracy depends of course on the system resolution given above.

Errors in the optical recording system can degrade this accuracy and must be reduced or taken into account. Signal-to-noise ratios above 1-to-1 allow an effective expansion of the pulse bandwidth by computer processing after the data is taken and accuracies greater than the single pulse accuracy can be achieved. Statistics can be used on a collection of several pulses to remove the system errors and reduce standard deviation of the measured image distance from the true one. Finally the geometry of the relative positions of the aircraft and the targets strongly affects the accuracy to which relative absolute distances between targets can be determined and converted to planar projections; i.e., horizontal distances as required in surveying.

To eliminate errors due to non-linearity of the sweep speed of the CRT in the optical recorder, a calibration of the sweep is made during the time of the experiment. A 5-MHz square wave is less than 10^{-9} seconds, which corresponds to about 6 in. of radar range. The grating formed by the square wave is used as a measurement of an elapsed time between radar range echoes. Although the square wave is not recorded during the recording of the target echoes, the drift of the CRT characteristics between the square wave recording and the echo recording is negligible.

As mentioned, the signal-to-noise ratio of the target echoes is very important, as it affects the ultimate resolution of the system. Since system noise and noise from other sources falling within the radar bandwidth are at least 15 to 20 dB below the reflected clutter level, only the clutter need be considered. The signal-to-clutter ratios are the cross-section ratios given in Section II-B-2 above. The effect of the signal-to-clutter ratio on resolution is given by

$$r_{\text{with processing}} = \frac{r_{\text{single pulse}}}{\sqrt{\text{signal/clutter}}}$$

The equation states that digital processing can be performed on a single pulse to decrease the effective spot size by an amount proportional to the square root of the signal-to-clutter ratio. A digital matched filtering process can be performed to increase the effective pulse bandwidth and improve resolution. The frequency spectrum of the pulse is not limited to the nominal bandwidth of 10 MHz, but extends to higher frequencies at low amplitude levels. This is a

statement of the theorem that a temporally finite signal has an infinite frequency spectrum. When the signal-to-noise levels are high enough so that these "Fresnel ripples" of the pulse spectrum can be detected, they may be used in the matched filtering process to obtain a smaller spot size.

The geometry of the radar ranging system must be analyzed in order to obtain the radar target separation from the data. Using a Cartesian coordinate system as shown in Fig. 3, the position of the plane can represent the center; i.e., (0, 0, 0) and the two targets represented by (x_1, y_1, h_1) and (x_2, y_2, h_2) respectively where x is the along track or azimuth coordinate of the target, y is the ground-range coordinate, and h is the altitude (relative between aircraft and target). The ground range distance between the targets is then

$$d = \sqrt{(x_2 - x_1)^2 + (y_2 - y_1)^2}$$

Normally the flight path is chosen to be perpendicular to the line formed by the targets which would give $x_2 = x_1$, but in the event that the path is not perpendicular, the azimuth coordinates cannot be neglected.

The data gives the radar ranges, r_1 and r_2, to the two targets at each pulse along the azimuth track where the targets are in the antenna beam. The radar range to a point on the ground is given by

$$r = \sqrt{x^2 + y^2 + h^2}$$

The parameter of interest is the ground range y which is given by

$$y = \sqrt{r^2 - x^2 - h^2}$$

The radar range r is found from the absolute time delay, T, of the echo and the speed of light:

$$r = \frac{TC}{2}$$

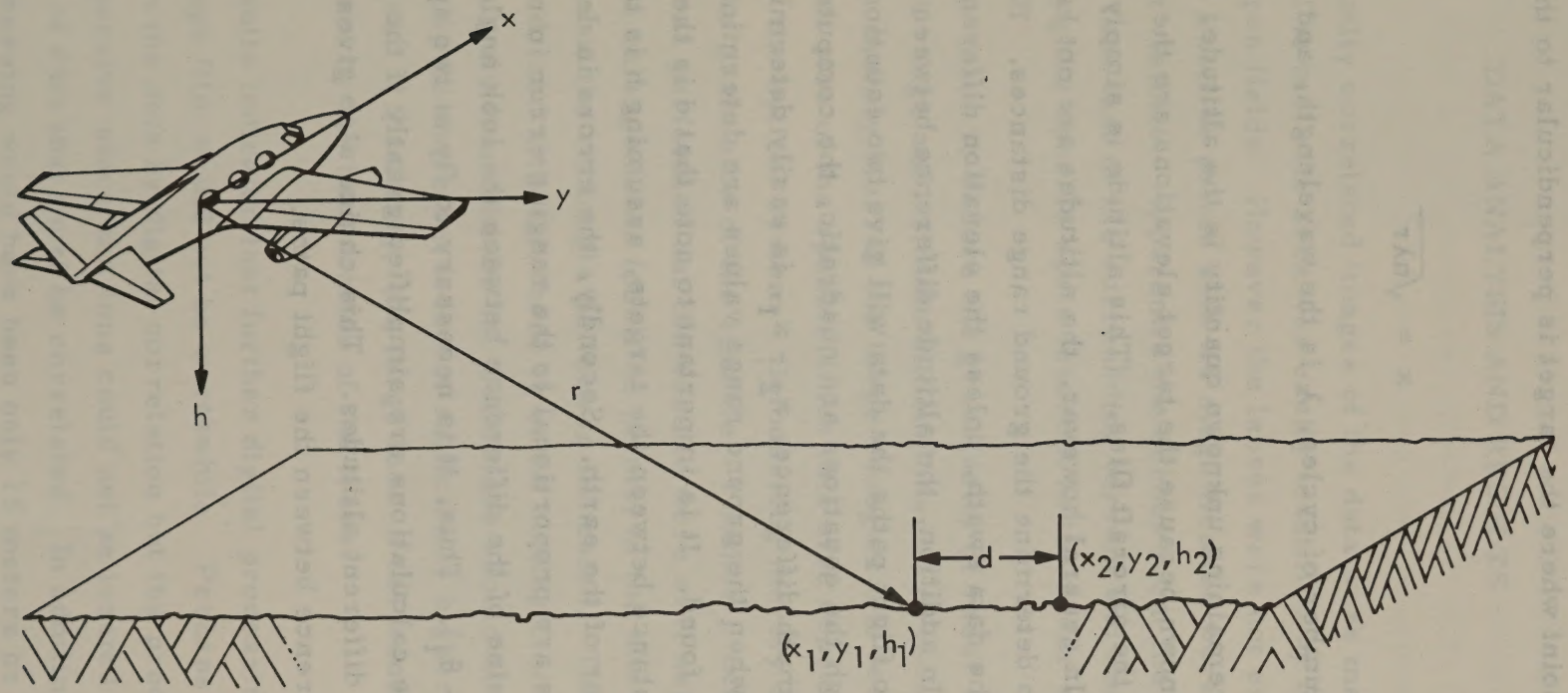

Fig. 3. Cartesian coordinate system

The azimuth distance, x, is found from the number of Doppler cycles from 0 Doppler (the point where the target is perpendicular to the flight path of the airplane) by

$$x = \sqrt{n\lambda r}$$

where n is the number of cycles, λ is the wavelength, and r is the range.

The only remaining unknown quantity is the altitude, h. In some cases the altitude, h, is known because the target elevations are the same as the point of land over which the aircraft flies. (This altitude is simply the range to the first surface echo.) In general however, the altitudes are not known and two flights are necessary to determine the ground range distances. Both flights must include both targets in the data swath, unless the elevation difference between the targets is known. In addition, the altitude difference between the paths must be known. With two flight paths the data will give two equations in the two unknowns, y and h. Although the equations are quadratic, the computer can solve them easily. The azimuth difference, $x_2 - x_1$, is easily determined from the equation for x above and when the ground range values are determined, the ground distance, d, can be found. It is important to note that d is the true horizontal projection of the distance between the targets, assuming h is taken along an axis through the center of the earth. Secondly, the errors in determining y and h in the two equations are proportional to the ranging error in r and inversely proportional to the sine of the difference between the look angles of the two flight paths, sine $(\theta_2 - \theta_1)$. Thus, it is necessary to fly at two appreciably different look angles. The calculations are simplified greatly if the two paths are over the same line at different altitudes. This choice also gives a direct measure of the altitude difference between the flight paths.

SECTION III

DATA ANALYSIS AND RESULTS

The first optically correlated images of the data were made and inspected on June 27, 1974. The test site area was easily identified by Rock Creek Reservoir and the open fields. However the lenses were not evident in the original negatives. Positive prints with X8 magnification were made but the lenses were still not visibile. Apparently the echoes from the lenses were not significantly higher than that of the surrounding terrain and the points were unrecognizable among the speckle spots inherent in the radar system.

An attempt was made to reduce the granularity of radar image by reprocessing the data with range and azimuth dimensions out of focus. This technique, however, merely blurred the large recognizable features and did little to alter the spot size of the speckle since this size depends only on the bandwidth passed by the optical system. Defocussing merely changes the grain pattern, not the grain size of the speckle. Further processing with reduced bandwidth was performed but the results were still negative Included here are some of the enlargements (positive prints) of the site area and the approximate location of the rectangle pattern is indicated. The level field areas are easily recognized, and although there is some clutter from these areas, the lens echoes, particularly from the 24-in. reflectors should have shown up. The lens echo may actually be there but it is not sufficiently higher than the clutter to be easily recognized. Similarly, the large lens in the wooded area is apparently masked out by the backscatter of the trees.

The above results indicated that further digital processing of either the data film or the image film would not be worthwhile. Perhaps the lenses could have been located in the data by digital correlation but the process would have been relatively expensive since the lens could not be located optically to reduce the quantity of data that must be correlated. In addition the accuracy yielded by such processing would have been only 15 meters or more since the signal-to-clutter ratio was apparently no more than unity.

Figure 4 shows inlargements of the radar imagery. The first (a) is the south to north run; the long narrow field and the rectangular field indicate the area where the lenses were. The second (b) is the east to west run where Rock Creek Reservoir (Fig. 1) is easily recognized. The third (c) shows the attempt to reduce the speckle by defocussing the data.

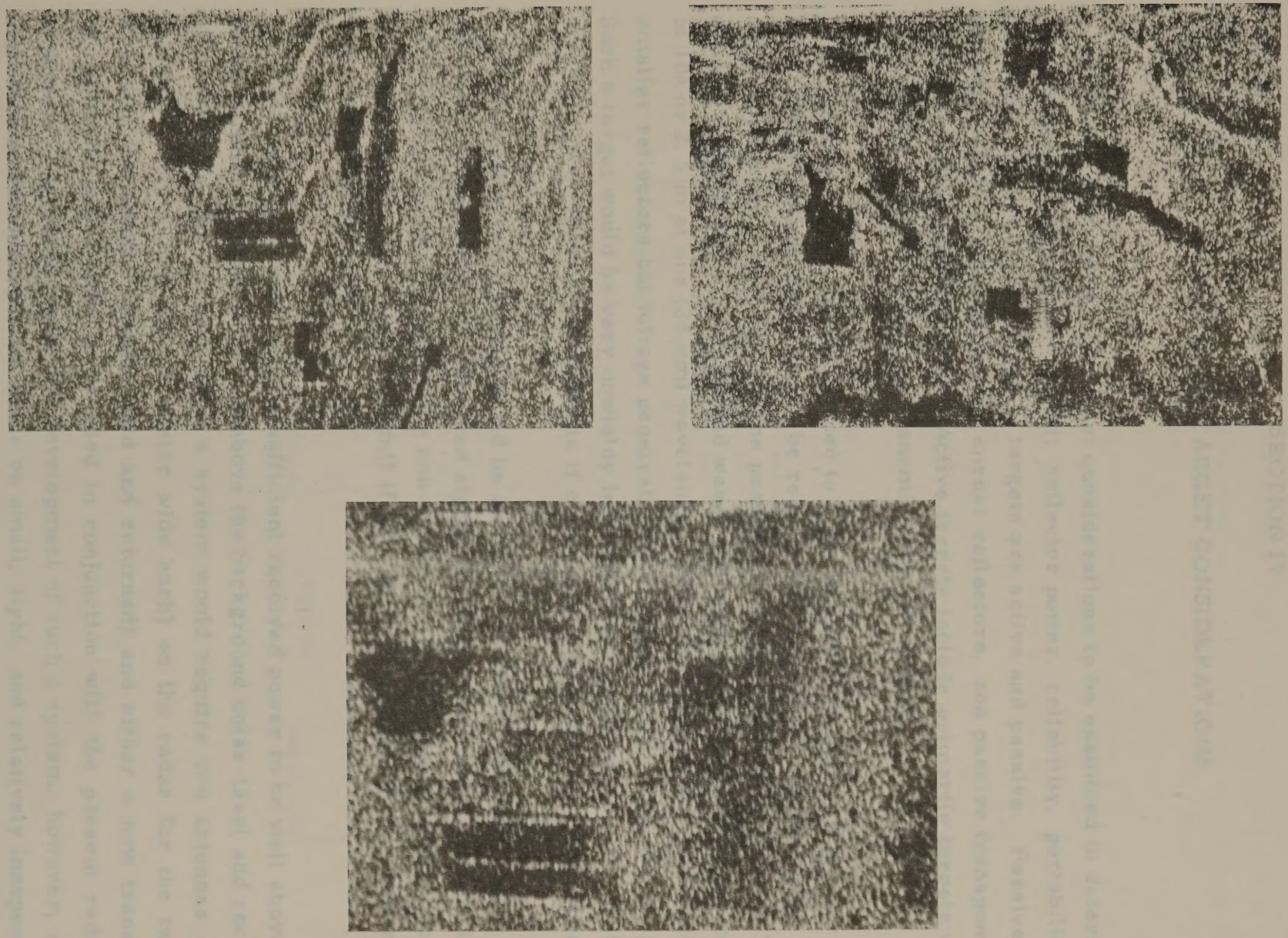

Fig. 4. Enlargements of radar imagery

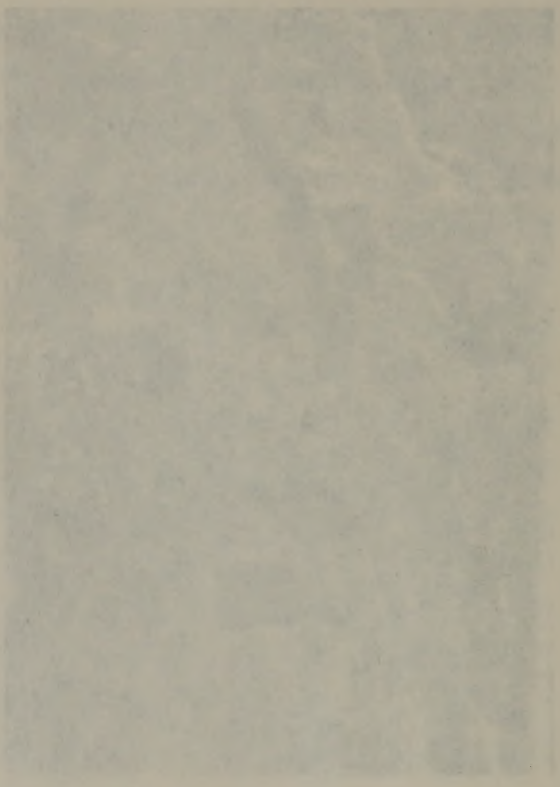

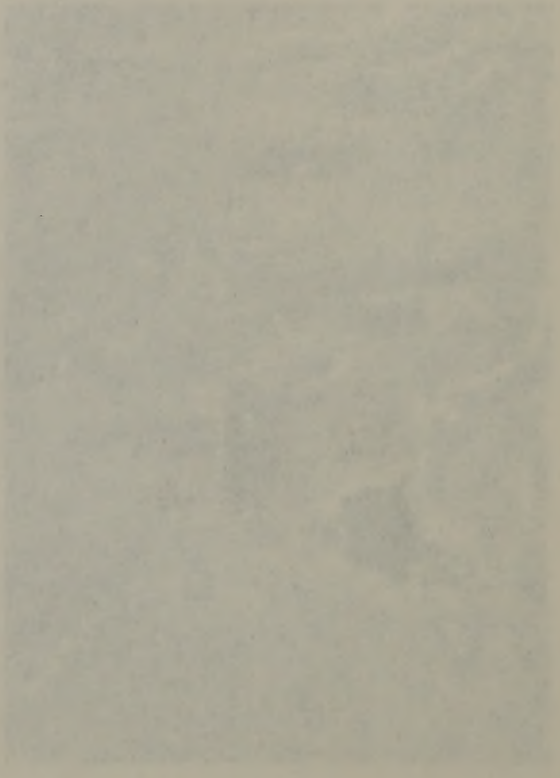

SECTION IV

ALTERNATE TARGET CONSIDERATIONS

There are several important considerations to be examined in determining what type of target should be used: reflector power, reliability, portability, and cost. The two basic types of targets are active and passive. Passive targets include Luneberg lenses, corner reflectors, and passive transponders (i.e., no signal amplification). Active targets include primarily targets which amplify the reflected signal or transmit their own signal.

Corner reflectors are limited to a 90° acceptance angle. A cluster of four, placed back to back, would be required to provide 2π steradians of solid-angle coverage to include the possible flight paths of the airplane To achieve colimation of the reflected wave, the reflectors should be on the order of 10λ or 2.5 m at our (25 cm) wavelength. Shorter wavelengths would require smaller reflectors but foliage penetration decreases rapidly with wavelength. Such a target would be very unwieldy in the field and perpendicularity of the sides would be difficult to maintain if collapsible type reflectors were made.

A passive transponder would be an ideal solution if sufficient power were received by the device. A received signal could be multiplied (i.e., shifted upward in frequency) by a passive non-linear device. A single antenna could be used to both receive and transmit if a circulator arrangement as shown in Fig. 5 were to be used.

The system would require sufficient received power to be well above the noise level in the multiplier and above the background noise-level and receiver noise-level in the radar. Such a system would require two antennas (approximately 1 meter long by 1/2 meter wide each) on the radar for the two different frequencies (transmitted and returned) and either a new transmitter or receiver would have to be used in conjunction with the present radar system. Time and cost for the development of such a system, however, are significant: the transponder would be small, light, and relatively inexpensive;

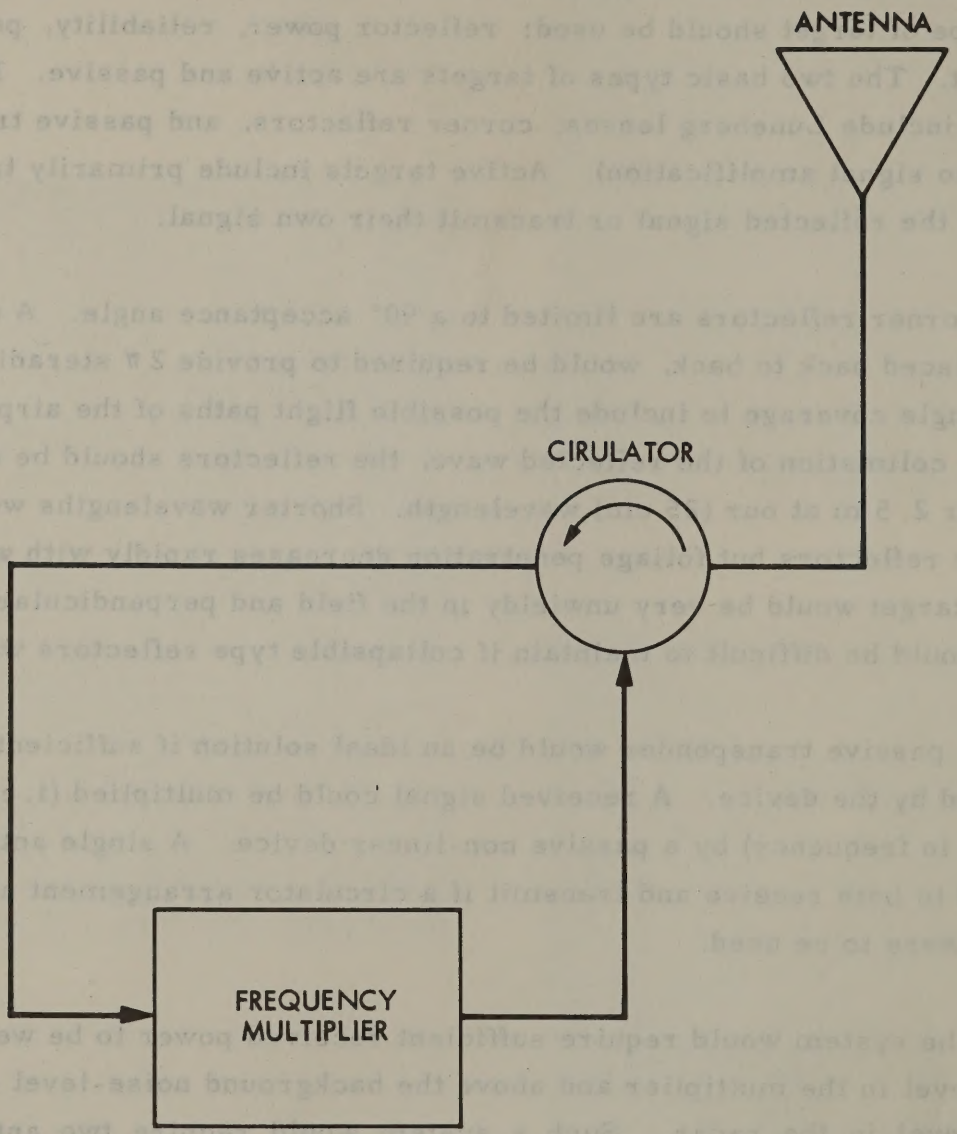

Fig. 5. Passive transponder

there are no batteries or other power system to burn out; the background clutter from other targets is virtually eliminated by receiving at a frequency different from the transmitted one.

Active transponders could provide stronger echoes than Luneberg lenses but the required signal amplification is considerable. A 36-in. Luneberg lens has an effective radar cross-section of 86 sq. m at L-band, while a dipole antenna has a cross-section of $0.12\ \lambda^2$ or 0.007 sq. m. To merely match the performance of the large lens, a gain of 10^4 would be required. In a real-time transponder it is also necessary to isolate the received signal from the transmitted signal by at least the system gain. A system which uses only a single antenna and a circulator would be limited to a system gain equivalent to the isolation of the circulator or about 20 dB. To achieve a gain of 40 or 50 dB, separate antennas would have to be used and isolation between them achieved by opposite polarization. Antennas with larger cross-sections than dipoles could possibly be used but isolating the two becomes a problem especially when one considers that they have to be very broad beamed (wider than say 100°).

An active transponder which multiplied the frequency of the returned signal would not have the isolation problem. This system would be similar to a passive multiplier with the addition of an active amplification stage or stages. This system requires a power source and is the most expensive choice, but may be the only system that will work (Ref. Appendix C).

SECTION V

CONCLUSIONS

The radar as an imaging system worked well and land features and test sites were easily recognized. However, the echoes from the reflectors were not detected. An analysis of the data indicates that ths scintillation of the echoes from the forested surface and countryside produced echo peaks that were equal to or exceeded the echoes from the reflectors. The scintillation amplitude can be reduced by averaging adjacent resolution cells but the apparent resolution is reduced. The conclusion is that the reflector cross-section must not only exceed the average radar cross-section of the terrain but it must exceed the root-mean square of the scintillating cross-section. Methods for reducing the scintillation are available, they generally require excess bandwidth or extended synthetic apertures.

The ability of the imaging radar to see passive reflectors in a clutter background created by forests or rocky terrain is limited by the bandwidth of the radar. Existing systems could probably succeed in areas where the terrain is relatively smooth such as ice fields or desert areas.

To succeed in forested areas, our recommendation would be to investigate the use of second harmonic transponders wherein the mode of operation would be to simultaneously record the second harmonic echo on one channel and the fundamental echo on a second channel. Then the marker location could be referenced to the surface features observed in the image. The second harmonic transponder echo would not be required to compete with clutter from the fundamental, only the cosmic or thermal noise which is several orders of magnitude less than clutter level. Thus, the detection and location would be relatively simple. The complexity would be in the design of the second harmonic transponder. A brief system description of a second harmonic transponder is given in Appendix C.

APPENDIX A

RADAR DESCRIPTION AND RADAR SIGNAL FILM CHARACTERISTICS

I. RADAR SYSTEM DESCRIPTION

A simplified functional block diagram of the radar is shown in Fig. A-1. A stable local oscillator is the "clock" for the system. Its frequency is 5 MHz and its long term stability is about 1 part in 10^{10}. Such frequency stability is required to maintain phase coherency of the radar system over the integration period of the synthetic aperture which can be several seconds. This frequency is used in the logic and timing controls which, as the name implies, supplies the gates, triggers, etc. for all components of the system. The oscillator is multiplied by 243 to produce 1215 MHz the rf carrier frequency. The clock is also multiplied to 60 MHz in the "chirp" generator. Here a pulse travels through a dispersive line to produce a 20 MHz linear frequency sweep of 2 μs duration. Normally only half of the "chirp" is used by the exciter/modulator to modulate the travelling wave tube (TWT).

When the pulse is transmitted, the low noise amplifier in the receiver is turned off to prevent the leakage in the circulator from burning out the receiver. The received signal (echo) is amplified and mixed with the carrier frequency resulting in a video signal with a frequency spectrum from 0 to 10 MHz. After amplification, the echo is recorded on a CRT whose sweep is triggered by the timing controls. Consecutive pulses (which occur at a rate of 1000 pps at a ground speed of 250 m/s) are recorded with about 2-1/2 to 1 overlap on the photograph in the optical recorder. The sweep length is nominally 25 mm and the time is 50 "s.

Figures A-2 through A-7 give a pictorial description of the actual radar hardware. Figure A-2 consists of drawings of the major system components. Figure A-3 shows the interconnections for these components. Figures A-4, A-5, and A-6 show the transceiver, instrumentation rack, and the antennas respectively, as they are mounted for operations in the NASA Ames CV990.

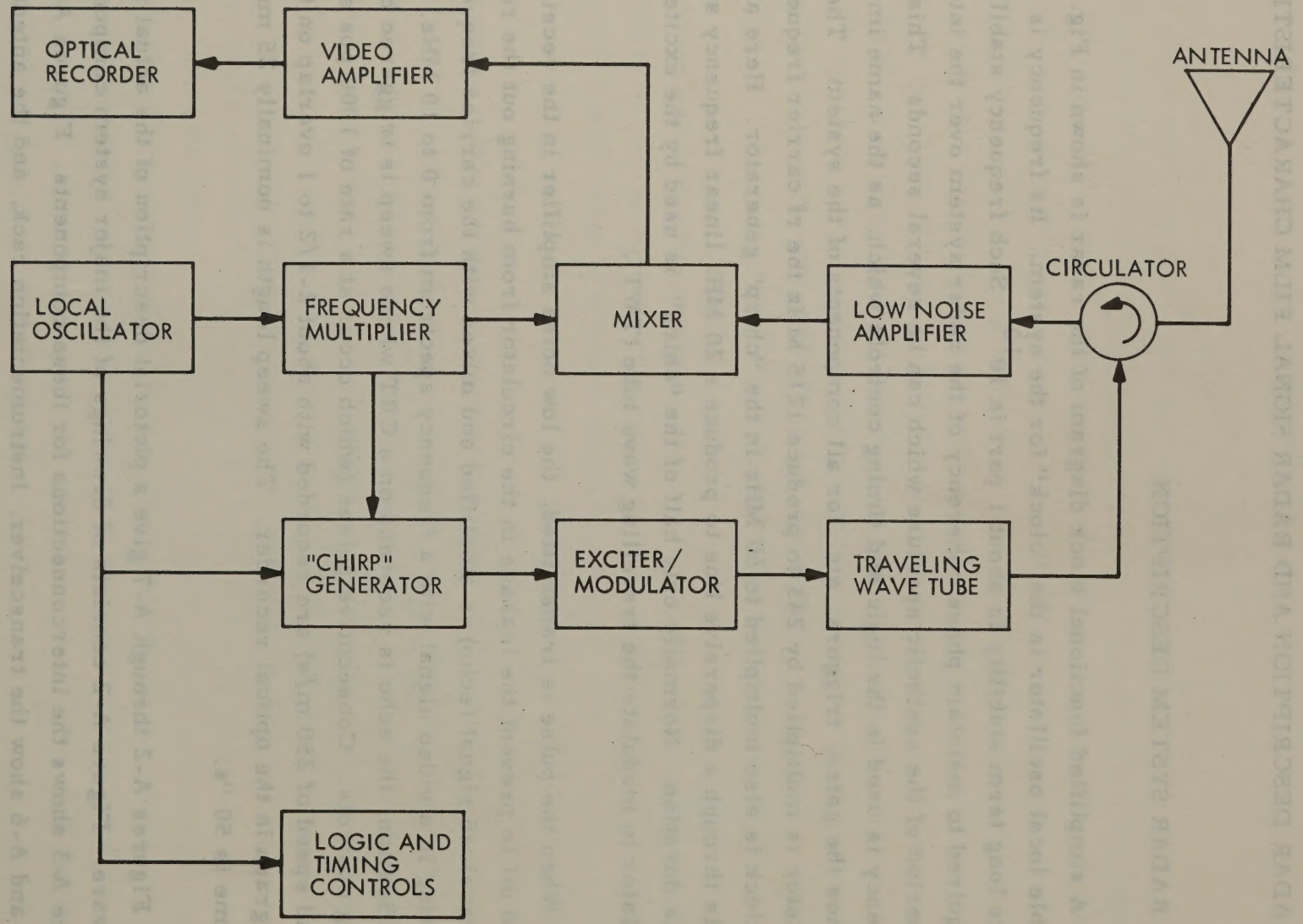

Fig. A-1. Simplified functional block diagram of L-band radar system used in BLM experiment

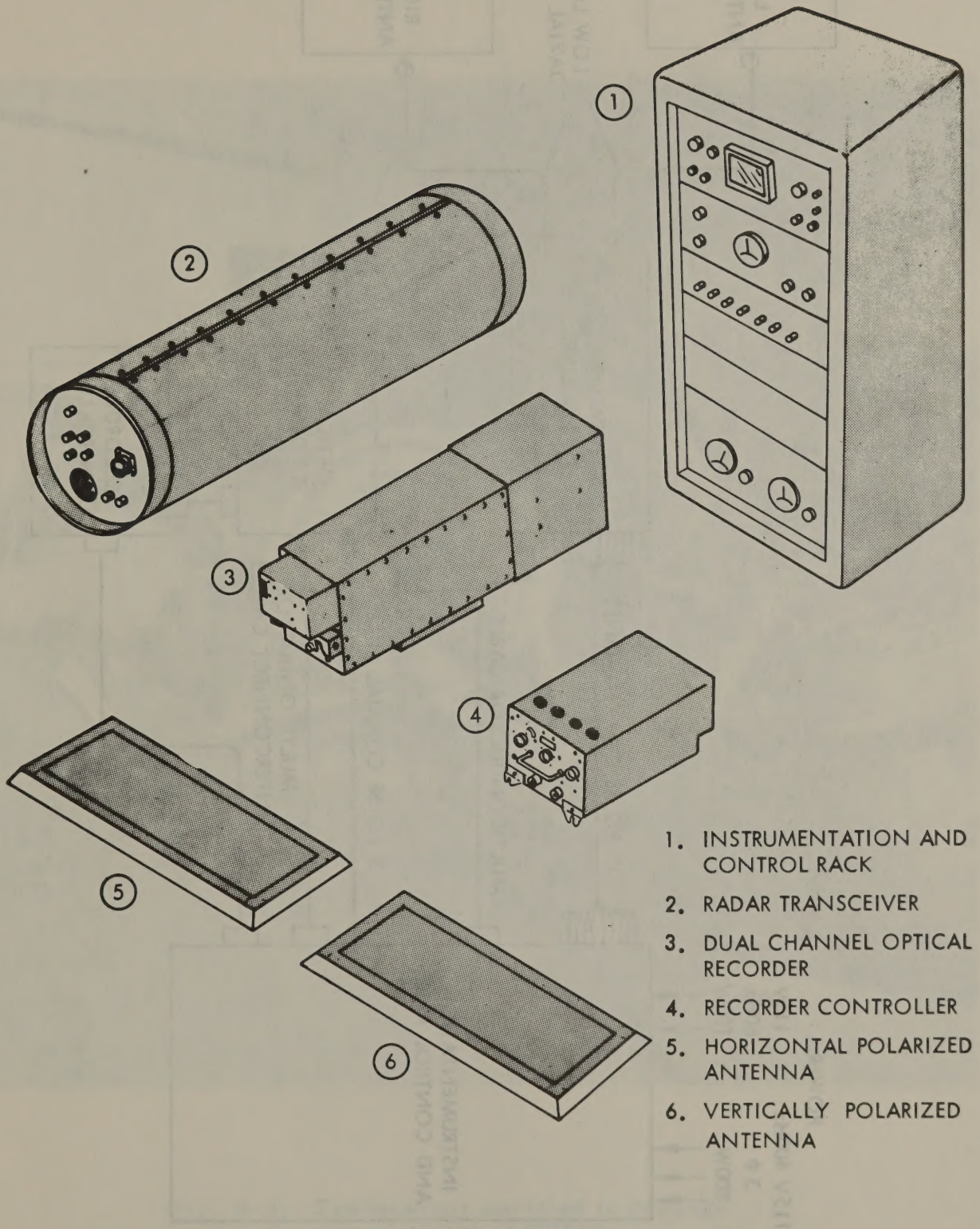

Fig. A-2. JPL coherent imaging radar system hardware

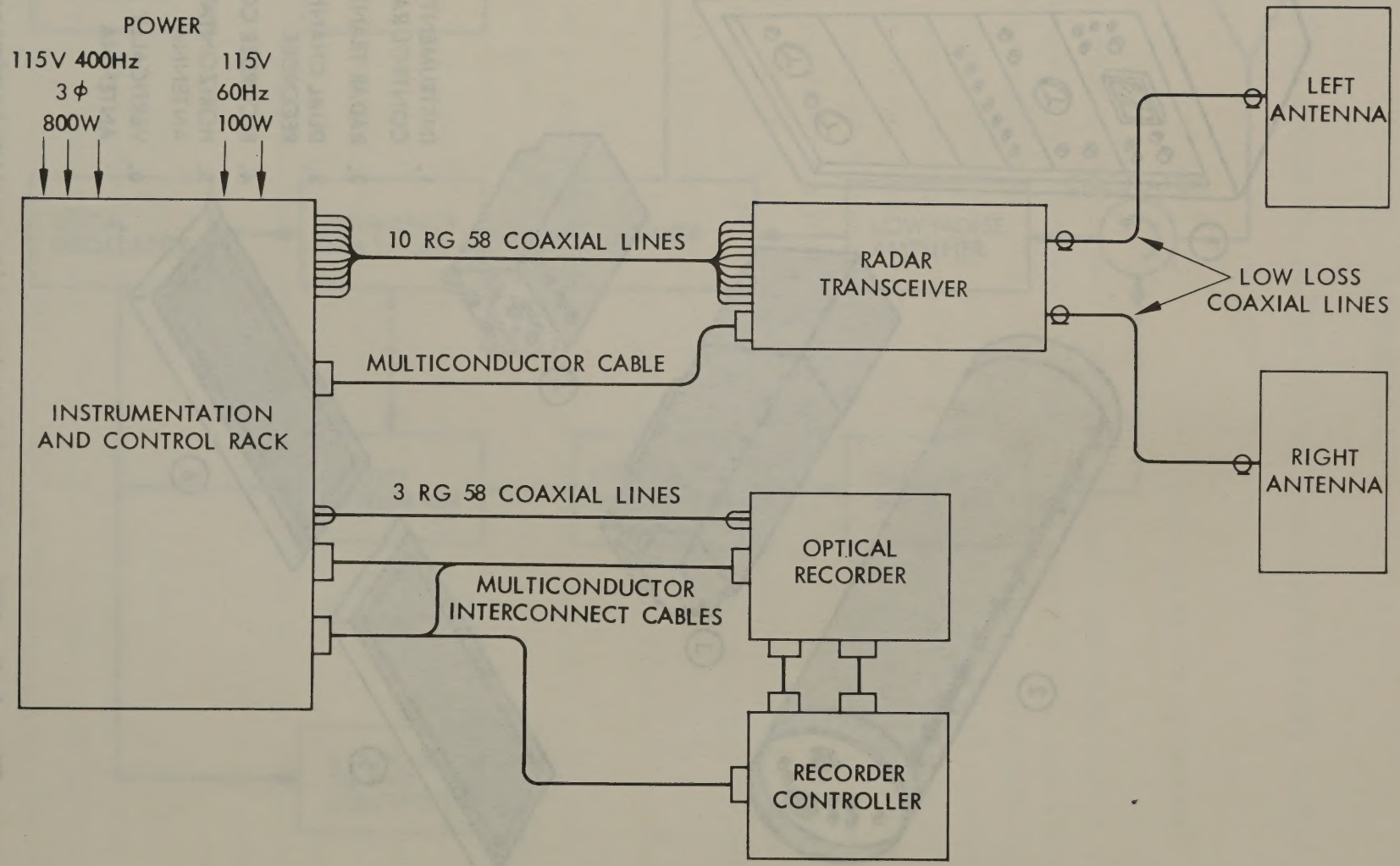

Fig. A-3. JPL coherent imaging radar system interconnect diagram

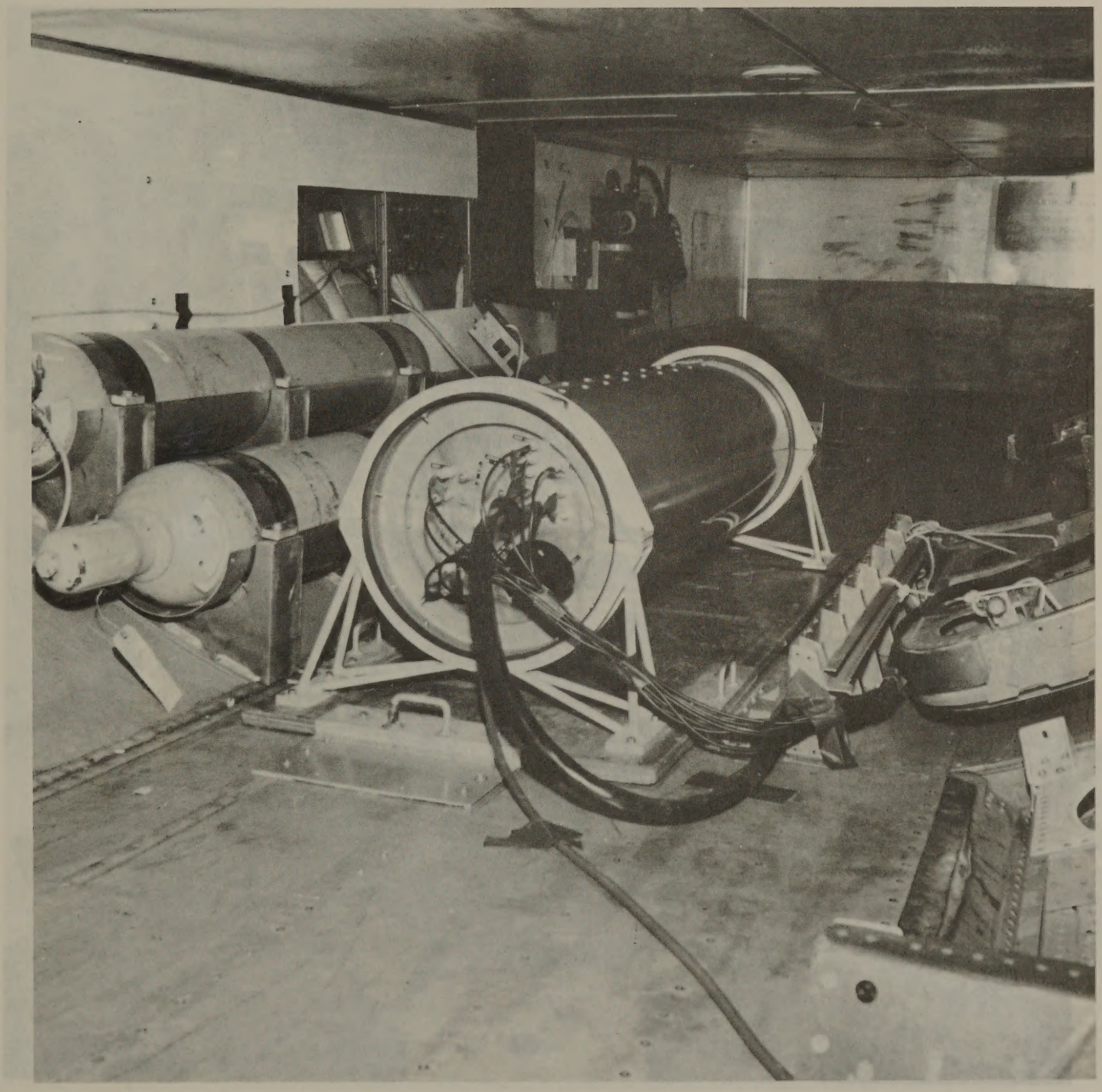

Fig. A-4. Transceiver mounted in baggage compartment of CV990

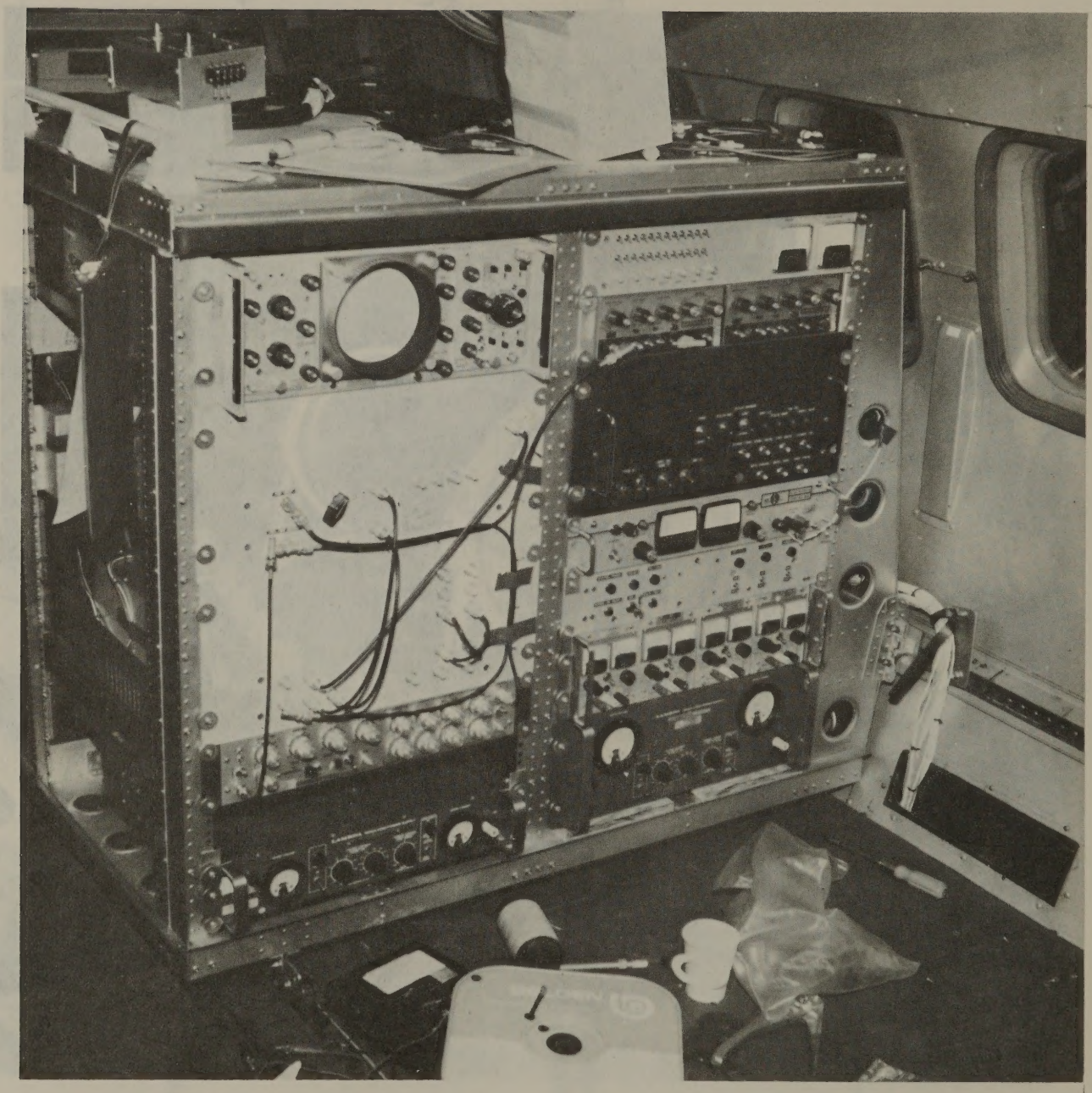

Fig. A-5. Instrumentation and control rack in passenger compartment of CV990

Fig. A-6. Antennas mounted on baggage door of CV990

II. SIGNAL FILM CHARACTERISTICS

Tne chirped pulse transmitted by the radar has the form

$$f(t) = \cos(2\pi f_o t + \pi B t^2) \qquad \text{(A-1)}$$

where F_o is rf carrier frequency and B is rate of the frequency sweep.

The temporal frequency modulation of the chirp is converted to a spatial density modulation when the pulse is mixed with the rf and recorded on the CRT. For an echo from a particular point target at radar range r, the phase of the local oscillator that is mixed with the returned echo is

$$p(t) = 2\pi f_o \frac{2r(t)}{C} \qquad \text{(A-2)}$$

where C is the speed of light. The mixer essentially subracts this phase from the echo. The range r may be expressed in terms of the normal slant range r_o and the azimuth distance from the target $(x - x_o)$ where x_o is the location of the target by

$$r(t) = \sqrt{(X(t) - x_o)^2 + R_o^2} \qquad \text{(A-3)}$$

Since the azimuth antenna beam is narrow so that $x - x_o$ is usually much less than r_o the quadratic approximation may be made:

$$r(t) \approx r_o + \frac{x(t) - x_o^2}{2r_o} \qquad \text{(A-4)}$$

The azimuth position x(t) is converted to spatial dimensions on the film by

$$x(t) \rightarrow \frac{V_f}{V_a} x \qquad \text{(A-5)}$$

where v_a is the aircraft velocity and v_f is the film velocity. The range coordinate, y, on the film is determined from the sweep speed, v_s, of the recorder by

$$t \rightarrow \frac{y}{v_s} \qquad \text{(A-6)}$$

combining relations Eq. A-1 through A-6 the transmission function for a point target on the signal film is

$$t(x, y) = t_o + m\cos \frac{2\pi v_a^2 (x - x_o)^2}{\lambda_r r_o v_f^2} + \frac{\pi B y^2}{v_s^2} \qquad \text{(A-7)}$$

where t_o is the bias density, m is the percentage modulation, and λ_r is the radar wavelength.

Rewriting Eq. (A-7) as

$$t(x, y) = t_o + m\cos \frac{\pi}{\lambda_\ell} \frac{(x - x_o)^2}{f_a} + \frac{y^2}{f_c} \qquad \text{(A-8)}$$

where f_a and f_q are the azimuth and range (or chirp) focal lengths respectively of the data film when it is illuminated by a coherent plane wave of wavelength λ_ℓ. A photograph of a section of data film with point targets and the corresponding image is shown in Fig. A-7. Note the long elliptical lines characteristic of Eq. (A-8). The focal lengths are given in terms of radar parameters by

$$f_a = \frac{\lambda_r r_o v_f^2}{2\lambda_\ell v_a^2} \qquad \text{(A-9)}$$

and

$$f_c = \frac{v_s^2}{B\lambda_\ell} \qquad \text{(A-10)}$$

Typical examples are (with $\lambda_r = 0.25$ meters, $r_o = 10^4$ m, $v_f = 0.01$ m/s, $\lambda_\ell = 0.6 \times 10^{-6}$ m, $v_a = 250$ m/s, $v_s = 500$ m/s and $B = 10^{13}$ cycles/s^2):

$$f_a = 3.1 \text{ meters}$$

$$f_c = 0.039 \text{ meters}$$

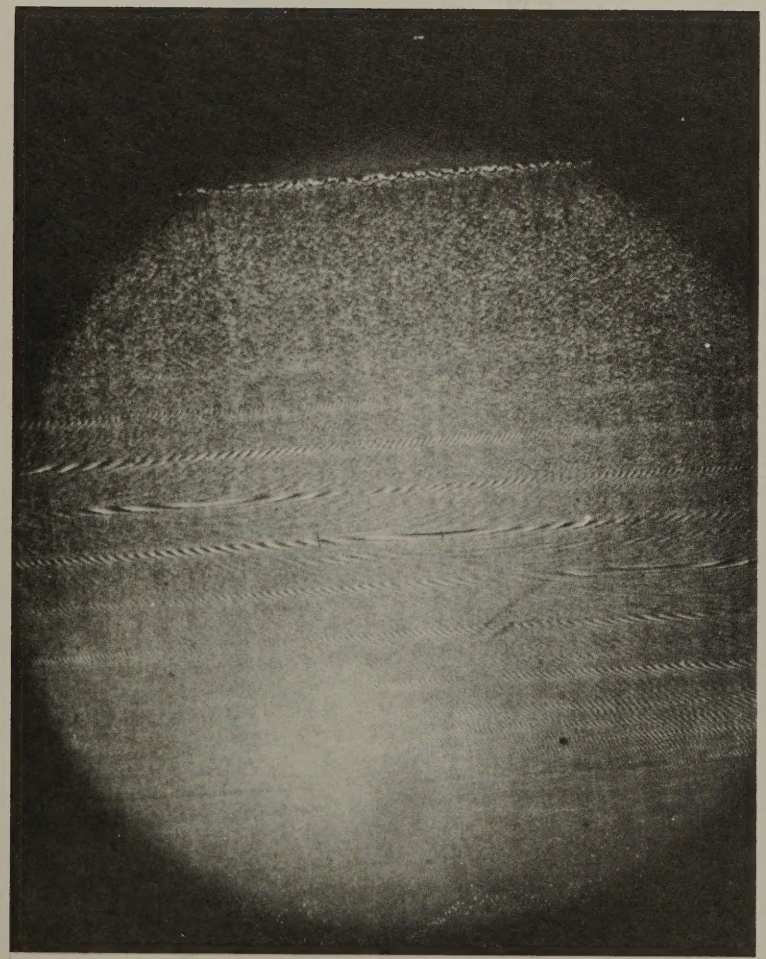

SIGNAL FILM

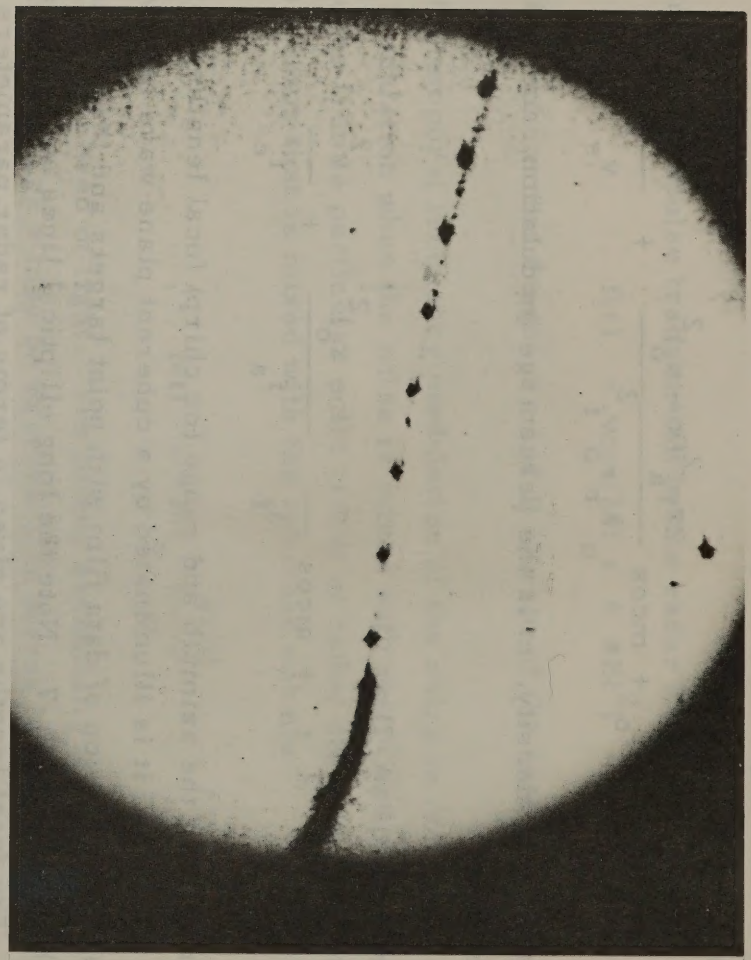

IMAGE FILM

Fig. A-7. Point target responses Atherton Bridge
San Francisco Bay

APPENDIX B

PROCESSOR THEORY AND OPERATION

I. INTRODUCTION

The primary function of the JPL optical processor is to generate map films from data films recorded in synthetic aperture radar systems. The radar system records the amplitude and phase of radar pulse echoes on photographic film. When a chirped pulse is used, the film will exhibit focal properties similar to a holographic recording. However the focal properties in the two dimensions (range and azimuth) are different, and the signal-to-noise ratio is quite low. The processor performs optical filtering to remove the noise and the "dc" component, and anamorphic imaging to obtain a focused image of the recorded terrain.

The standard configuration of the processor is the tilted-plane mode of operation. In this mode the input and output planes are tilted with respect to the optical axis. A confocal, spherical lens pair images the range and azimuth focal planes, and a 3-lens cylindrical telescope demagnifies the azimuth dimension. Frequency filtering is done at the back focal plane of the first spherical lens. A block diagram of the processor optical system is shown in Fig. B-1. The system can be broken down into the fore-optics system and the primary optical system.

II. PROCESSOR SYSTEM DESCRIPTION

A. FORE-OPTICS

The light source of the processor is a HeNe laser that generates 15 mW at 6328 Å. The laser cavity resonates in the TEM_{oo} mode and emits a linearly polarized, Gaussian beam. The diameter of the power level $(\frac{1}{e^2})$ of the beam is 1.1 mm and the bandwidth is approximately 500 MHz.

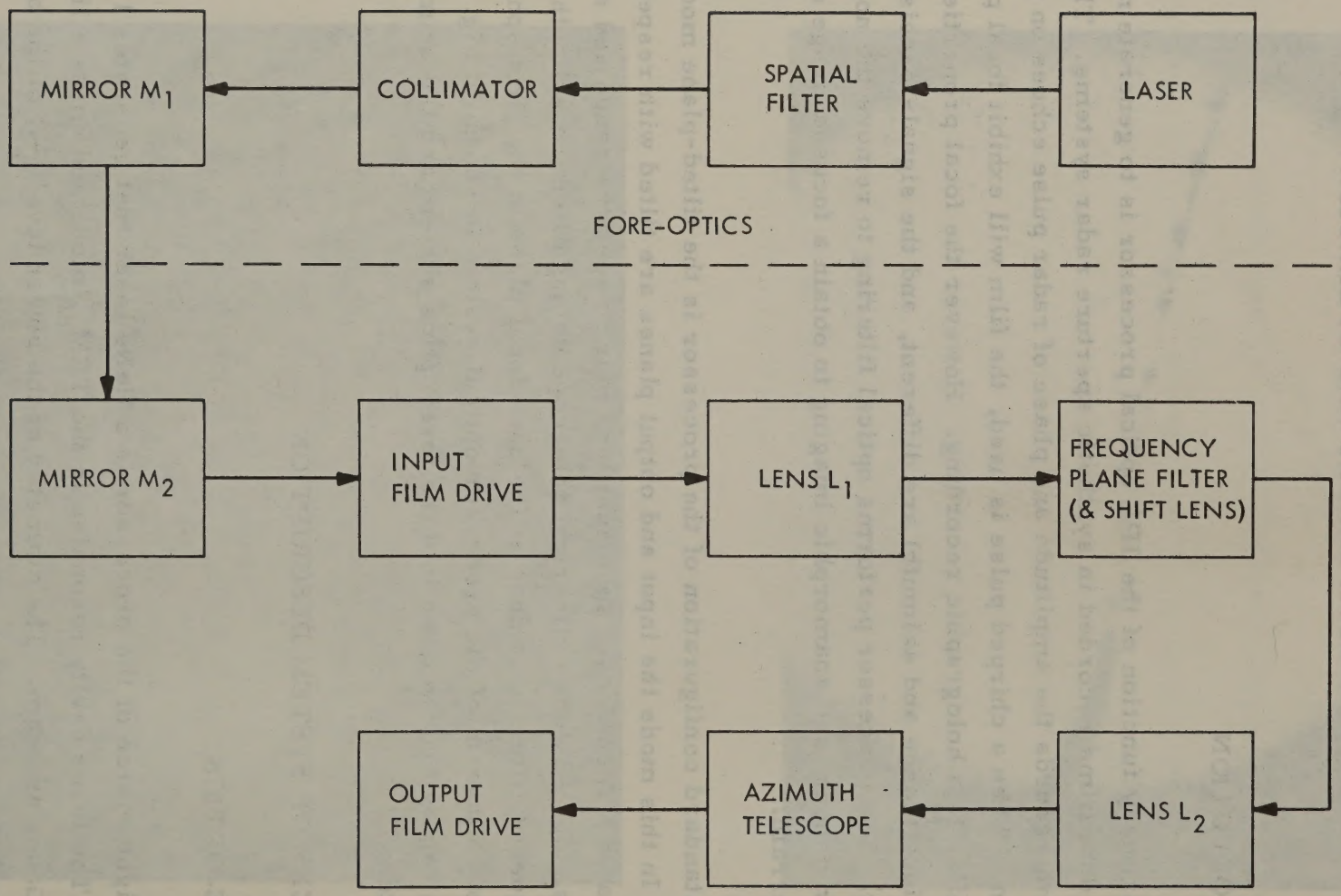

Fig. B-1. Primary optical system

The relative positions of the components in the spatial filter and collimator are shown in Fig. B-2. The spatial filter is composed of a microscope objective lens and a pinhole. The pinhole is located at the back focal point of the objective, blocking out spatial noise in the laser beam. Thus a "clean" diverging spherical wave emerges from the filter.

The collimator is composed of two elements spaced approximately 21 in. apart. The first element is a convex-concave negative lens with a 29-in. focal length and a 1-1/2-in. aperture. The second element is a plano-convex lens with a 28-1/2-in. focal length and a 6-1/2-in. aperture. When the full aperture of the input lens is illuminated by the diverging wave from the filter, the output will be a 6-1/2-in. diameter plane wave. The wave is then reflected through a 90° bend by mirror M_1 toward mirror M_2, the first element of the primary optical system. Both mirrors are 8 in. in diameter and flat to 1/4 wave.

B. PRIMARY OPTICAL SYSTEM

Mirror M_2 bends the beam through another 90° angle and can be adjusted to provide an offset illumination angle in range and/or azimuth. It is desirable to have the center frequency of the spatial frequency band in both dimensions aligned with the optical axis to insure optimum use of the lens apertures. Thus, if a data film has equal positive and negative frequencies in both range and azimuth, the center of the band is zero frequency in both dimensions. Hence, the film should be illuminated with an on-axis beam. However, if the data has equal positive and negative frequencies in azimuth but runs from 0 to some positive frequency in range, a range offset would be used.

The input film drive transports the data film to be processed. The film passes through a liquid gate which removes phase noise caused by emulsion irregularities. The along axis position of the film drive is determined by the range focal length of the data film. The tilt angle of the drive depends upon both the slope of the azimuth focal plane and the demagnification of the azimuth telescope.

Lens L_1 is the first of a spherical lens pair. The positions of the input and output data planes with respect to lenses L_1 and L_2 are shown in Fig. B-3.

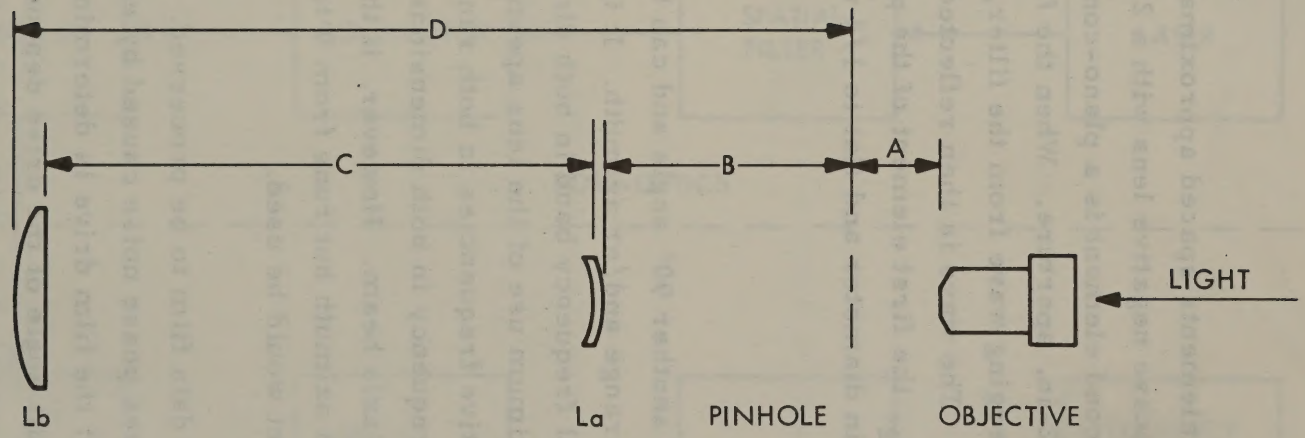

A: DISTANCE FROM OBJECTIVE TO ITS FOCUS (WHERE PINHOLE IS) WILL VARY WITH OBJECTIVE USED

B: DISTANCE FROM PINHOLE TO FRONT VERTEX OF LENS La IS 9.775"

C: DISTANCE FROM BACK VERTEX OF La TO FRONT VERTEX OF Lb IS 21.650"

D: DISTANCE FROM PINHOLE TO BACK VERTEX OF Lb IS 32.675"

Fig. B-2. Relative positions of spatial filter and collimator components

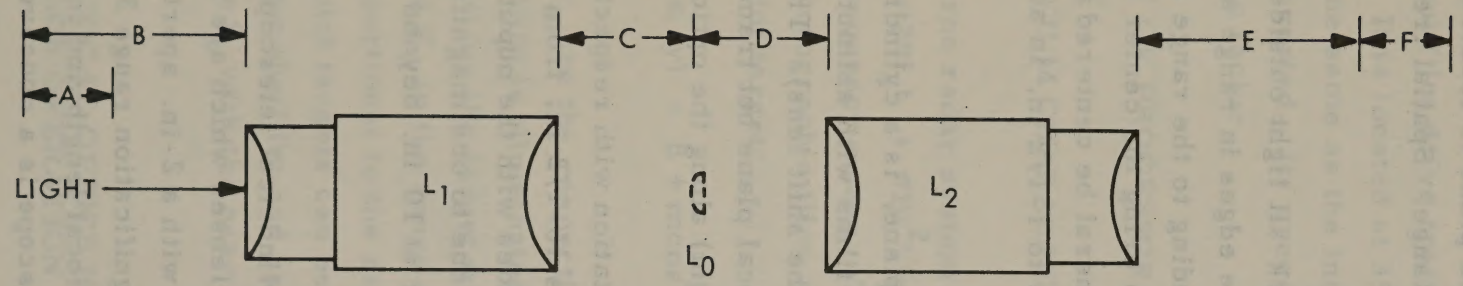

A: DISTANCE OF INPUT DATA (RANGE FOCAL PLANE OF SIGNAL FILM) FROM INPUT FOCAL PLANE OF L_1 IS 10.000"

B: INPUT FOCAL PLANE OF L_1 IS 25.171" FROM FRONT FLANGE

C: OUTPUT FOCAL PLANE OF L_1 IS 16.674" FROM BACK FLANGE

D: INPUT FOCAL PLANE OF L_2 IS 16.637" FROM FRONT FLANGE. WHEN SHIFT LENS IS USED, D BECOMES 16.968"

E: OUTPUT FOCAL PLANE OF L_2 IS 25.127" FROM BACK FLANGE

F: IMAGE OF RANGE FOCAL PLANE IS 9.971" FROM OUTPUT FOCAL PLANE OF L_2

Fig. B-3. Input and output data

Its aperture is 8 in. and its effective focal length is 31 in. Its input focal plane is approximately 25 in. from its front flange and the output focal plane is 16-1/2 in. from the back flange. The input data plane is located 10 in. behind the input focal plane or 15 in. from the front flange. Spatial frequency spectrum of the data occurs at the back focal plane.

The frequency plane filter is used to block all light outside the bandwidth of the data to be processed. Two pairs of knife edges in range and azimuth are adjusted to the rectangular aperture corresponding to the range and azimuth bandwidth. Since illumination offset is used to bring the center of the bandwidth along the optical axis, the rectangle will in general be centered about the optical axis. The rectangle is continuously adjustable to 1-1/2 in. in azimuth and 4 in. in range.

The shift lens, located at the frequency plane, is a cylindrical lens with power in the azimuth direction. It is used for films with azimuth focal lengths that are too long to allow processing (without the shift lens). The shift lens does not reduce the tilt angle of the azimuth focal plane but translates it in the negative direction (opposite the direction of light) along the optical axis.

Lens L_2 is identical to L_1 with its orientation with respect to light direction reversed. That is, its input focal plane is 16-1/2 in. from its front flange. It is located so that its input focal plane coincides with the ouput focal plane L_1. This combination forms a telescope with one to one magnification. A filtered image of the input data field will occur at 10 in. beyond its output focal plane, or 35 in. behind its back flange.

The azimuth telescope is a three lens cylindrical telescope used to demagnify the azimuth image. There are two lenses which are alternates for the first element of the telescope. The first, with a 2-in. aperture (in azimuth) and a 8-in. focal length, is used for the demagnification range 3 to 9. The second has a 3-1/2-in. aperture and a 25-in. focal length and is used for the range 9 to 25. The second element of the telescope is a concave-concave lens with a minus 1-1/2-in. focal length and a 1/4-in. aperture. The last element is a triplet lens with a 1-1/2-in. focal length and a 1/2-in. aperture. The

azimuth image will usually occur within a few inches of the output focal plane of the last lens.

The output film drive transponrts photographic film to be exposed by the output image. It is located at 35 in. beyond the back flange of L_2 and its tilt angle will be the same as the input drive except in the opposite direction since the image is inverted. Its speed will be that of the input drive divided by the demagnification factor.

II. THEORY OF PROCESSOR OPERATION

A. RADAR FILM CHARACTERISTICS

An airborne radar system transmits a continuous series of short pulses of the form $\cos(2\pi f_o t + \pi B t^2)$ where f_o is the RF frequency and B is the rate of the linear frequency sweep. The echoes of the pulses are coherently recorded by a CRT on photographic film, resulting in the following transmission function for an ideal point target:

$$T(x, y) = b + m\cos \frac{2\pi}{\lambda_\ell} \frac{(x - x_o)^2}{F_a + sy_o} + \frac{(y - y_o)^2}{F_r} \qquad \text{(B-1)}$$

where x_o and y_o are the respective azimuth and range film coordinates of the target. If the film is illuminated with a coherent plane wave of wavelength λ_ℓ, the "zone plate" for the target will focus the beam at a distance $(F_a + sy_o)$ in the azimuth and F_r in the range directions. The azimuth focal length, $F_a + sy_o$, is linearly proportional to the range coordinate, y_o. Thus a data film with a collection of point targets can be described as having a range focal plane a distance F_r from the film and an azimuth focal plane that slopes away from the film at an angle θ_o with the near focus at a distance F_a. As depicted in Fig. B-4, $\tan\theta_o = s$.

B. GEOMETRICAL OPTICS INTERPRETATION OF PROCESSOR OPERATION

The spherical lens pair, called the range telescope, images the film (and hence its focal planes) as shown in Fig. B-5. The unity magnification

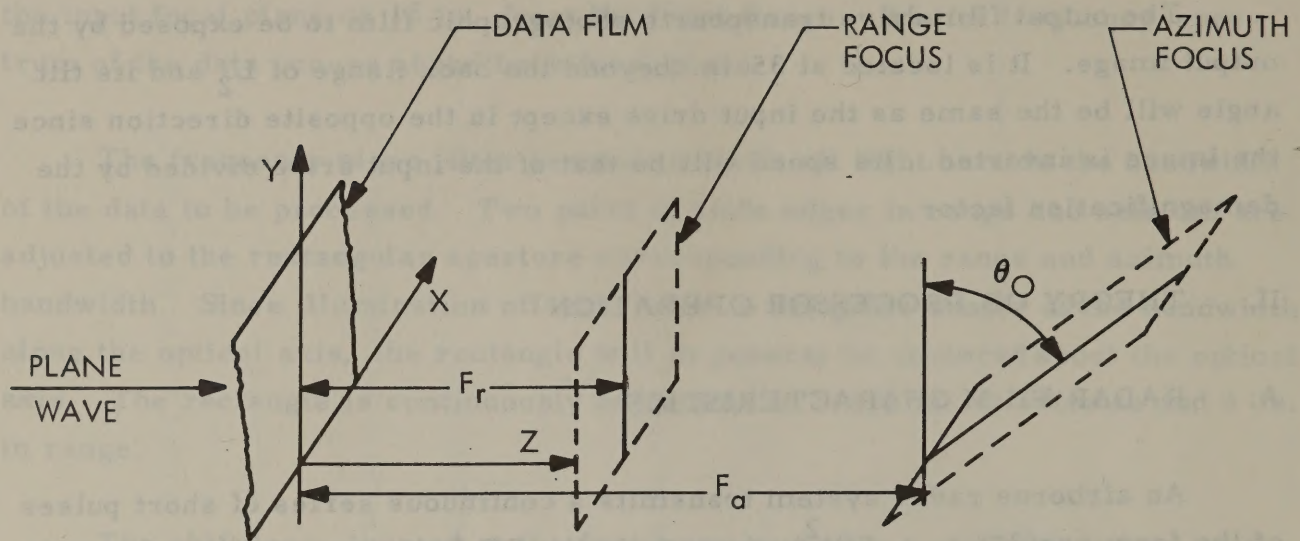

Fig. B-4. Range and azimuth focal planes

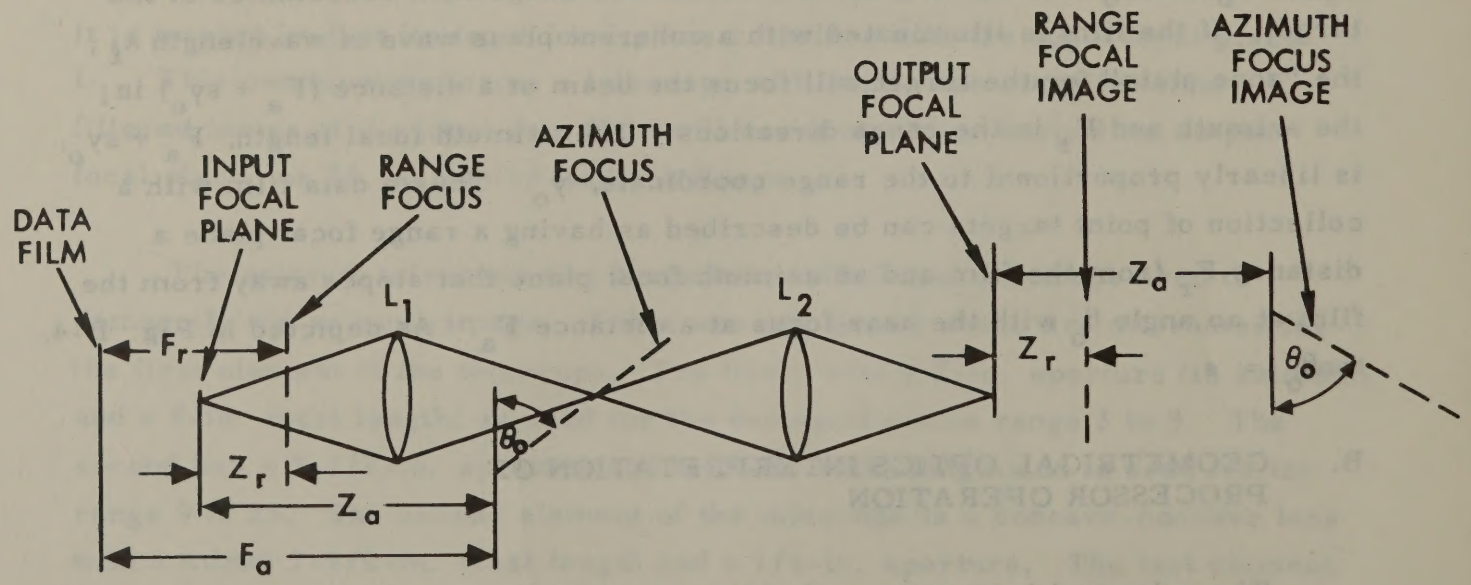

Fig. B-5. Range telescope

telescope translates the distance of an object from the input focal plane to the distance of the image from the output focal plane. The image will also be inverted about the optic axis (z-axis).

The azimuth telescope, composed of three cylindrical lenses, images in much the same manner as the spherical telescope with two basic differences - only the azimuth focal plane is affected, and demagnification occurs. Fig. B-6 illustrates that the input object to the telescope is the azimuth focal plane image projected by the spherical telescope. In this case, the distance of the object from the input focal plane, Z_o, and the distance of the image from the output focal plane Z_i, are related by:

$$Z_i = \frac{1}{D_L^2} Z_o \qquad \text{(B-2)}$$

and

$$\tan\theta_o' = \frac{1}{D_L^2} \tan\theta_o \qquad \text{(B-3)}$$

where θ_o' is the new tilt angle and D_L is the lateral demagnification of the telescope.

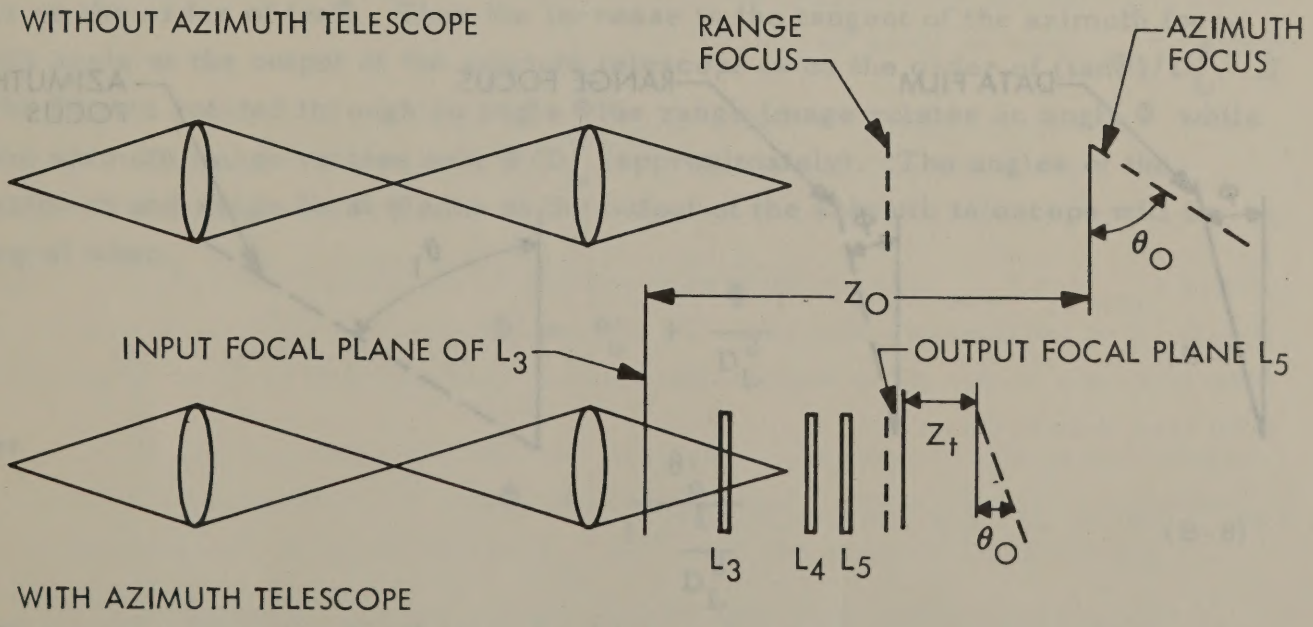

Fig. B-6. Azimuth telescope

Now the range and azimuth focal planes must be made to coincide to yield a focussed image. Consider a rotation of the input film through an angle Φ in the direction of the azimuth tilt, as shown in Fig. B-7. The range focal plane will also rotate to an angle Φ, while the azimuth focal plane will rotate to a new angle θ_1, whose tangent is given by:

$$\tan\theta_1 = \frac{s + \sin\Phi}{\cos\Phi} \qquad \text{(B-4)}$$

when the tilted film is imaged by the two telescopes, as shown in Fig. B-8, the range focal plane image will have a tilt angle Φ and the azimuth focal plane will have a tilt angle θ_1' defined by:

$$\tan\theta_1' = \frac{1}{D_L^2} \tan\theta_1 \qquad \text{(B-5)}$$

Note that for small angle , equation (B-4) may be written as an approximation:

$$\tan\theta_1 = s + \tan\Phi \qquad \text{(B-6)}$$

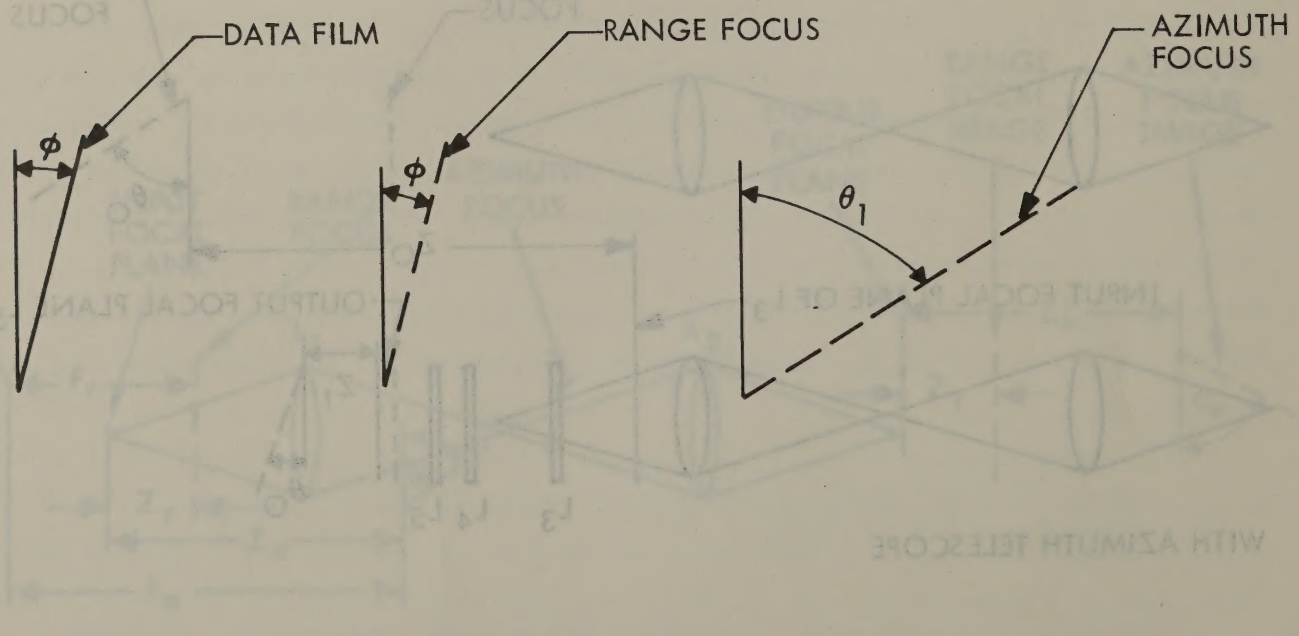

Fig. B-7. Data film tilt angle

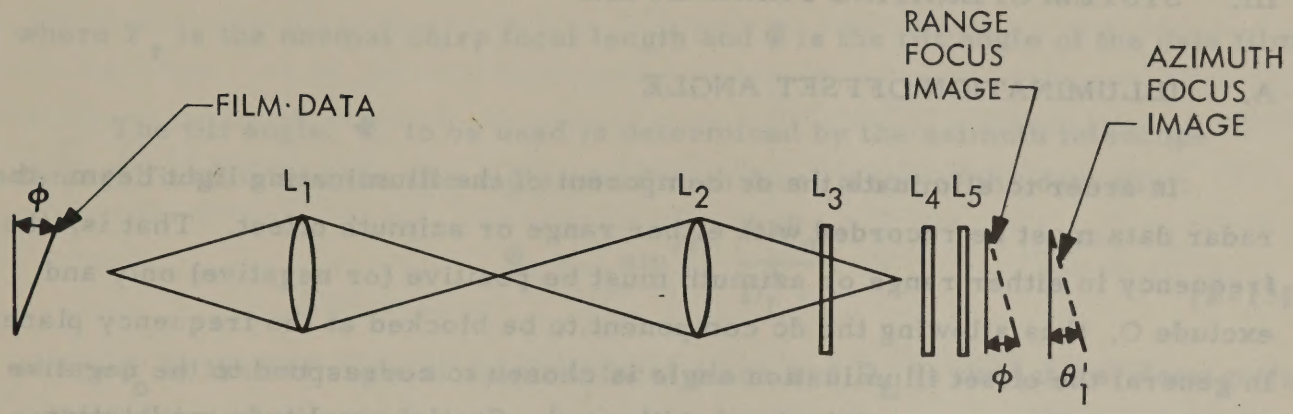

Fig. B-8. Equalizing range end azimuth focal plane angles

revealing that the increase in the tangent of azimuth focus tilt angle of the film is on the order of tanΦ. Thus the increase in the tangent of the azimuth focus tilt angle at the output of the azimuth telescope is on the order of $(\tan\Phi)/D_L^2$. If the film is rotated through an angle Φ the range image rotates an angle Φ while the azimuth image rotates only Φ/D_L^2 (approximately). The angles of the azimuth and range focal planes at the output of the azimuth telescope will be equal when

$$\Phi \simeq \theta'_o + \frac{\Phi}{D_L^2} \qquad \text{(B-7)}$$

or

$$\Phi \simeq \frac{\theta'_o}{1 - \frac{1}{D_L^2}} \qquad \text{(B-8)}$$

The exact expression for the required tilt angle is:

$$\Phi = \sin^{-1} \frac{S}{D_L^2 - 1} \qquad \text{(B-9)}$$

When this condition is met, the two focal planes can be moved into coincidence by a simple translation of the azimuth telescope along the z-axis.

III. SYSTEM OPERATING PARAMETERS

A. ILLUMINATION OFFSET ANGLE

In order to eliminate the dc component of the illuminating light beam, the radar data must be recorded with either range or azimuth offset. That is, the frequency in either range or azimuth must be positive (or negative) only and exclude O, thus allowing the dc component to be blocked at the frequency plane. In general the offset illumination angle is chosen to correspond to the negative of the center frequency of the bandwidth used. Spatial amplitude modulation diffracts a plane wave into an angle nearly proportional to the spatial frequency, as given by

$$\theta = \sin^{-1} \lambda_\ell f \tag{B-10}$$

where θ is the angle of the diffracted beam with respect to the input beam, λ_ℓ is the illuminating wavelength, and f is the spatial frequency. Thus the offset angle, θ_{off}, may be given by

$$\theta_{off} = - \frac{\sin^{-1} \lambda_\ell f_{min} + \sin^{-1} \lambda_\ell f_{max}}{2} \tag{B-11}$$

where f_{min} and f_{max} are the minimum and maximum spatial frequencies, respectively. For frequencies less than 120 cycles/mm and λ = 6328 Å, the inverse sine functions in the above expression may be approximated by their arguments with less than 0.1% error.

B. INPUT DATA FILM LOCATION

The position of the input data film is chosen so that its range focus will occur at 10.000 inches beyond the input focal plane of lens L_1. The range

(or chirp) focal length will change as a function of the tilt angle of the data. The tilted chirp focal length F_r' becomes

$$F_r' = F_r \cos\Phi \tag{B-12}$$

where F_r is the normal chirp focal length and Φ is the tilt angle of the data film.

The tilt angle, Φ, to be used is determined by the azimuth telescope demagnification and the tile angle of azimuth focal plane of the data film:

$$\Phi = \sin^{-1} \frac{\tan\theta_o}{D_L^2 - 1} \tag{B-13}$$

where θ_o is the tilt angle of azimuth focal plane and D_L is the lateral demagnification of the telescope.

C. FREQUENCY PLANE FILTER APERTURES

The range and azimuth apertures of the frequency plane filter are determined by the range and azimuth spatial frequency bandwidths, the wavelength of illumination, and the focal length of lens L_1. The aperture, A_f, for a given bandwidth is

$$A_f = F\lambda_\ell \Delta f \tag{B-14}$$

where F is the focal length of the lens, λ_ℓ is the wavelength, and Δf is the spatial frequency bandwidth. Note that a non-offset Doppler history with spatial frequency up to 50 cycles/mm has a 100 cycles/mm bandwidth because the history goes positive and negative in frequency.

D. SHIFT LENS

The use of a shift lens will be required if the focal length is too long to allow superposition of the range and azimuth focal plane images. A positive cylindrical lens of focal length, F_o, will shift the azimuth image in the z direction by an amount

$$Z_s = \frac{-F^2}{F_o} \tag{B-15}$$

where F is the focal length of L_1.

E. AZIMUTH TELESCOPE LENS POSITIONS

The azimuth telescope demagnification depends on the desired aspect ratio and, in some cases, upon the tilt angle of azimuth focal plane. When the data film has an aspect ratio of, say, 10, and an aspect ratio of 1 is desired for the map film, then the telescope demagnification will be 10. However, if this demagnification is not sufficient to reduce the azimuth tilt angle to less than 15°, then greater demagnification must be used. The upper limit of the telescope is $D_L = 25$, and if a greater D_L is required, another lens configuration must be used.

Once the required D_L is determined, the lenses are spaced according to the formulas

$$D_4 = \frac{F_4 F_5 D_L}{F_3} = .0903'' \times D_L \text{ for } L_{3A} \qquad \text{(B-16)}$$

$$D_3 = \frac{F_4^2}{D_4} = \frac{25''}{D_L} \text{ for } L_{3A} \qquad \text{(B-17)}$$

The distances D_2, D_3, D_4 are shown in Figure 9. F_3, F_4, F_5 are the focal length, or lenses L_3, L_4, and L_5 respectively.

The location of the azimuth focal image (without the azimuth telescope) with respect to the output focal plane of L_2 is

$$Z_a = 10.000'' - F_r' + F_a \qquad \text{(B-18)}$$

where F_r' is the chirp focal length and F_a is the azimuth focal length. The location of the azimuth focal image with respect to the input focal plane of L_3 is then

$$Z_i = D_2 + Z_a \qquad \text{(B-19)}$$

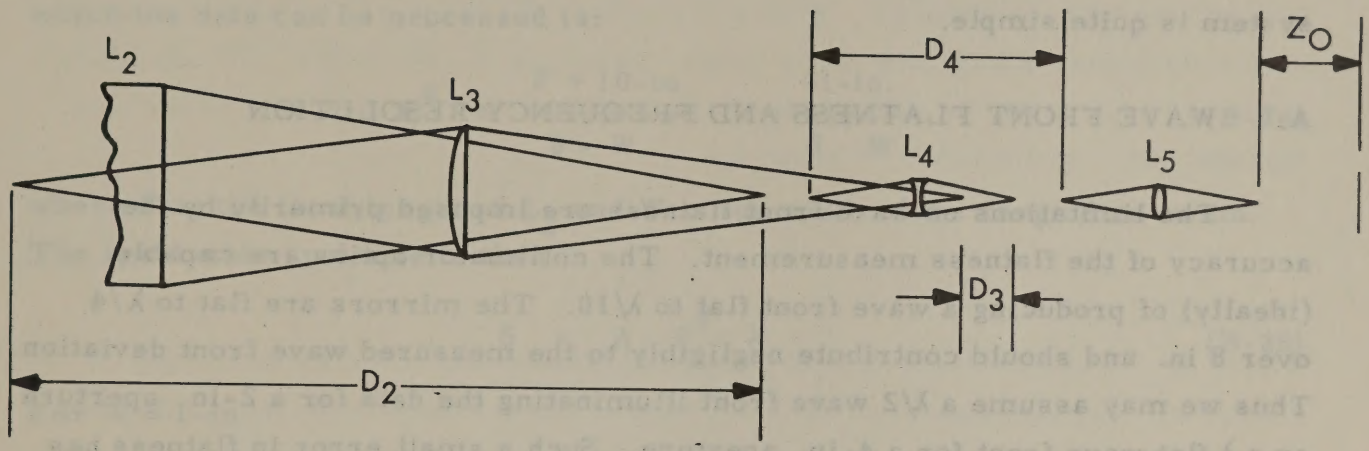

Fig. B-9. Azimuth telescope parameters

and the azimuth images will occur at Z_o where

$$Z_o = \frac{1}{D_L^2} Z_i + \frac{F_5^2}{D_4} \qquad \text{(B-20)}$$

All azimuth positions refer to mid-range azimuth focal lengths. If the mid-range of the data swath does not occur at the optical axis, additional telescope positioning will be necessary to find the azimuth focus.

F. OUTPUT FILM DRIVE

The output film drive is to be located a distance Z_o from the output focal plane of lens L_5. The tilt angle is exactly that of the input film drive except in the opposite sense. The direction of motion is the same as that of the input (since the image is inverted twice in azimuth). The output film speed is $1/D_L$ times the input speed. The exposure is proportional to D_L for a given input film speed and illumination.

IV. SYSTEM PERFORMANCE

The following performance analysis is based upon diffraction limited operation of the lenses. However, since the system is linear, inclusion of the effects of component irregularities on the overall performance of the system is quite simple.

A. WAVE FRONT FLATNESS AND FREQUENCY RESOLUTION

The limitations on wave front flatness are imposed primarily by the accuracy of the flatness measurement. The collimator optics are capable (ideally) of producing a wave front flat to $\lambda/10$. The mirrors are flat to $\lambda/4$ over 8 in. and should contribute negligibly to the measured wave front deviation. Thus we may assume a $\lambda/2$ wave front illuminating the data for a 2-in. aperture or a λ flat wave front for a 4-in. aperture. Such a small error in flatness has no effect on the processor resolution, but does limit its frequency resolving capability. A wave front deviation of $\lambda/2$ in 2-in. corresponds to an angular error, E_a, given by:

$$E_a = \frac{\lambda/2}{2''} \approx 6 \times 10^{-6} \qquad \text{(B-21)}$$

This angular error corresponds to a spatial frequency error of

$$E_f = \frac{E_a}{\lambda} \approx 10^{-2}/\text{mm} \qquad \text{(B-22)}$$

The frequency resolution imposed by the illuminated data aperture, A_d, is given by

$$f_{x_{res.}} = \frac{2}{A_d} = \begin{cases} 4 \times 10^{-2}/\text{mm for } A_d = 50 \text{ mm} \\ 2 \times 10^{-2}/\text{mm for } A_d = 100 \text{ mm} \end{cases} \qquad \text{(B-23)}$$

Thus frequency resolution is limited by the data aperture rather than the illuminating wave front. It is important to note that the aperture referred to is the span of the spatial frequencies involved. That is, if a frequency occurs over some distance on the film which is less than A_d, then the shorter distance must be used to calculate the frequency resolution.

B. RANGE RESOLUTION

The range resolution of the processor is limited by the output $F^{\#}$ at which the data can be processed. Since the range image occurs at 10-in. beyond the output focal point of L_2 and the effective aperture of L_2 is 8-in., the $F^{\#}$ at which the data can be processed is:

$$F^{\#} = \frac{F + 10\text{-in.}}{8 - W} = \frac{41\text{-in.}}{8 - W} \qquad \text{(B-24)}$$

where F is the focal length of L_2 and W is the width of the range data swath. The resolvable spot size is then

$$S = 2 \cdot F^{\#} \cdot \lambda \qquad \text{(B-25)}$$

For W = 1-in.

$$S = 2 \cdot \frac{41}{7} \cdot \lambda \approx 7 \times 10^{-3} \text{ mm} \qquad \text{(B-26)}$$

At the present time no recorder of ours can produce a chirp with a 7μ focus spot size. The actual resolution of the film-processor system is simply the convolution of chirp focus spot with the point-spread function of the optics. In the above illustrated case, the point-spread function is a sinc function with a main lobe 7μ wide (between zero crossings).

C. AZIMUTH RESOLUTION

The azimuth resolution is limited primarily by the azimuth telescope. The telescope is designed to operate at no lower than F/14 on the azimuth data. This $F^{\#}$ corresponds to a spot size of 17μ. In many cases the focus spot of the azimuth doppler history will focus to a spot which, when reduced by the D_L of the telescope, is smaller than 17μ, but the telescope is not capable of imaging the smaller spot. The resulting output will be a spot that is the convolution of the ideally smaller spot and the 17μ spot of the telescope.

D. RANGE CURVATURE LIMITATION ON COMBINED RANGE-AZIMUTH RESOLUTION

Every cycle of the Doppler history for a target represents a shift of the target one-half radar wavelength in range. The shift is toward far range on either side of zero Doppler. Hence the higher the Doppler frequency passed at the frequency plane, the more range curvature at the output. The azimuth spot size expressed as a function of the Doppler spatial frequency passed by the frequency plane filter is given by

$$S_a = \frac{2}{\Delta f_a} \tag{B-27}$$

where Δf_a is the azimuth spatial frequency bandwidth. The azimuth spatial frequency may be expressed as a function of the distance from zero Doppler on the film by

$$f_a = px \tag{B-28}$$

where p is the spatial frequency slope (in cycles/mm/mm) and x is the distance (from zero Doppler) in mm. The range curvature is given from the number of azimuth Doppler cycles on one side of zero Doppler. The number of cycles is just the integral of the frequency in expression

$$n = \frac{px^2}{2} \tag{B-29}$$

which may be expressed in terms of the Doppler frequency as

$$n = \frac{f_a^2}{2p} \tag{B-30}$$

The range curvature in radar space is then given by

$$C_r = \frac{\lambda r}{2} \cdot \frac{f_a^2}{2p} = \frac{\lambda_r f_a^2}{4p} \tag{B-31}$$

If we wish to process data with equal resolution in the azimuth and range dimension we would pass the Doppler frequency that resulted in a range curvature equal to the azimuth resolution. In the case where the curvature is still less than the chirp focus spot size, the only reason for reducing the azimuth spatial bandwidth would be to reduce noise. The range curvature is equal to azimuth spot size when

$$\frac{1}{A_r f_a} = \frac{\lambda_r f_a^2}{4p} \tag{B-32}$$

or when

$$f_a = \left(\frac{4p}{A_r \lambda_r} \right)^{1/3} \tag{B-33}$$

where A_r is the aspect ratio.

Note: $$p = \frac{2K_a}{\lambda_r R_o}$$

where K_a is the azimuth scale factor and R_o is the normal radar slant range.

E. DEPTH OF FOCUS

Depth of focus for any optical system is simply given by

$$D = 2 \cdot F^{\#2} \cdot \lambda \tag{B-34}$$

whre $F^{\#}$ is defined as the focal length divided by the effective aperture and λ is the wavelength of the light used. In the optical processor both the system and the data have $F^{\#}$'s. Naturally the depth of focus is given by the larger of the larger of the two $F^{\#}$'s. That is, the range $F^{\#}$ of the data will determine the range depth of focus and the azimuth depth of focus is determined by the larger of the data $F^{\#}/D_L$ and the azimuth telescope $F^{\#}$ (14). Of course since both range and azimuth are imaged, the output film drive must be positioned with error less than the smaller depth of focus.

APPENDIX C

A SECOND HARMONIC TRANSPONDER

The basic concept is to receive the transmitted pulse from the radar, double the frequency, amplify and transmit the signal. A functional diagram is shown below.

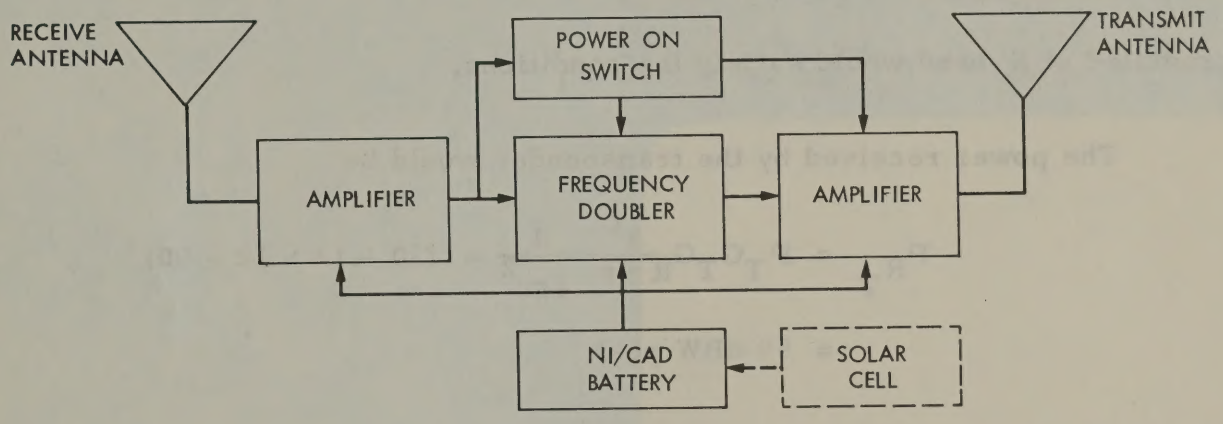

Example Parameters

Assume a 20 dB signal-to-noise ratio is desired.

$$\text{Noise} = kT\beta = -129 \text{ dBW}$$

$$\text{Signal} = \quad = -109 \text{ dBW}$$

$$P_S = P_T G_T \frac{G_R \lambda^2}{4\pi} \cdot \frac{1}{4\pi r^2}$$

Solve for P_T

$$P_T = \frac{P_S (4\pi r)^2}{G_T G_R \lambda_T^2} = \frac{-109 + 90}{13 - 18}$$

P_T = -14 dBW

So for a range of 10 km,

Transponder antenna G_T = 3 dB
Radar antenna G_R = 10 dB

so a peak power of 0.04 watts
or average power of

1.6 mW

radiated at S-band would satisfy the conditions.

The power received by the transponder would be

$$P_{R_T} = P_T G_T G_R \frac{\lambda^2}{4\pi} \frac{1}{4\pi r^2} = (30 + 13 \cdot 12 - 90)$$

$$= 59 \text{ dBW peak}$$

for 1 kW pulse transmitted.

The overall system functional diagram follows.

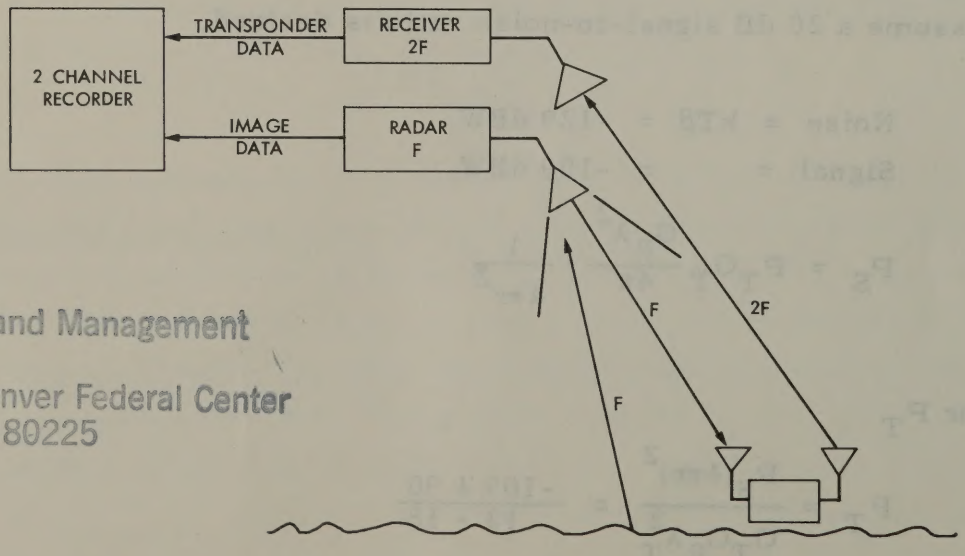

Bureau of Land Management
Library
Bldg. 50, Denver Federal Center
Denver, CO 80225

NASA — JPL — Coml., L.A., Calif.

Bureau of Land Management
Library
Bldg. 50, Denver Federal Center
Denver, CO 80225